



Electroweak Precision Measurements with ATLAS

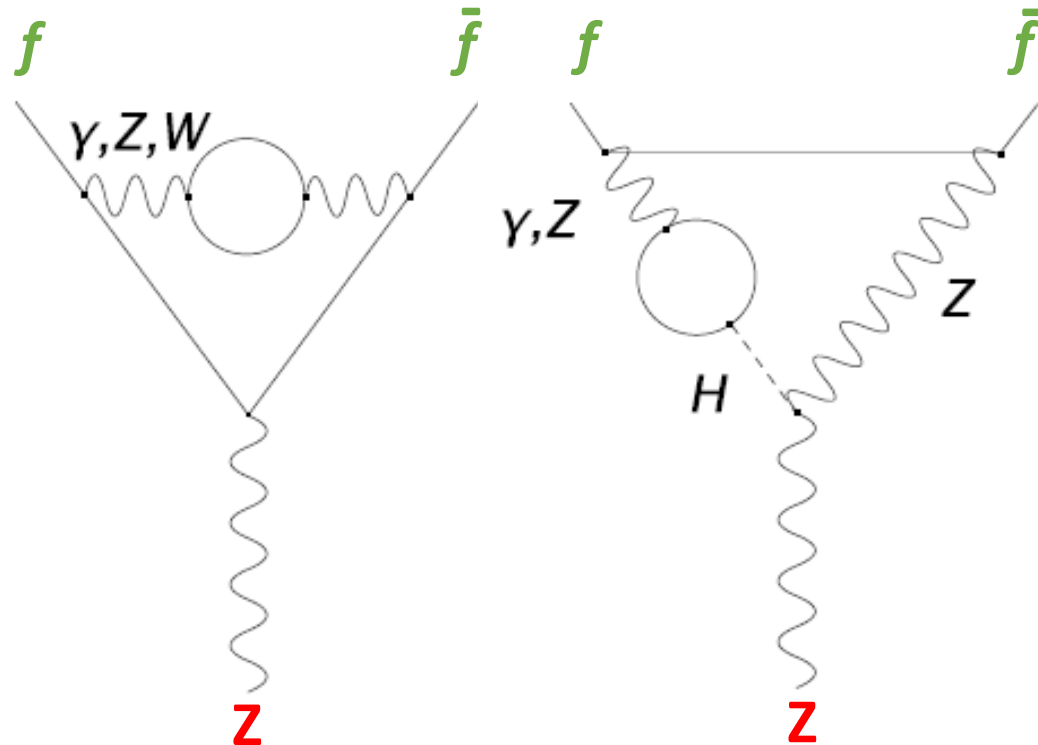
Maarten Boonekamp (CEA, IRFU),
on behalf of the ATLAS Collaboration

Outline

- Motivation : a window into the Higgs sector
- The weak mixing angle and associated measurements
- The W boson mass
- Vector boson scattering at high energy
- Current status and prospects

A window into the Higgs sector

Loop effects on gauge boson properties



L.O.:

$$g_V^{\text{tree}} \equiv (T_3^f - 2Q_f \sin^2 \theta_W^{\text{tree}})$$

$$g_A^{\text{tree}} \equiv T_3^f.$$



H.O.:

$$g_{Vf} \equiv \sqrt{\rho_f} (T_3^f - 2Q_f \sin^2 \theta_{\text{eff}}^f)$$

$$g_{Af} \equiv \sqrt{\rho_f} T_3^f,$$

$$\sin^2 \theta_{\text{eff}}^f \equiv \kappa_f \sin^2 \theta_W = \kappa_f (1 - m_W^2/m_Z^2)$$

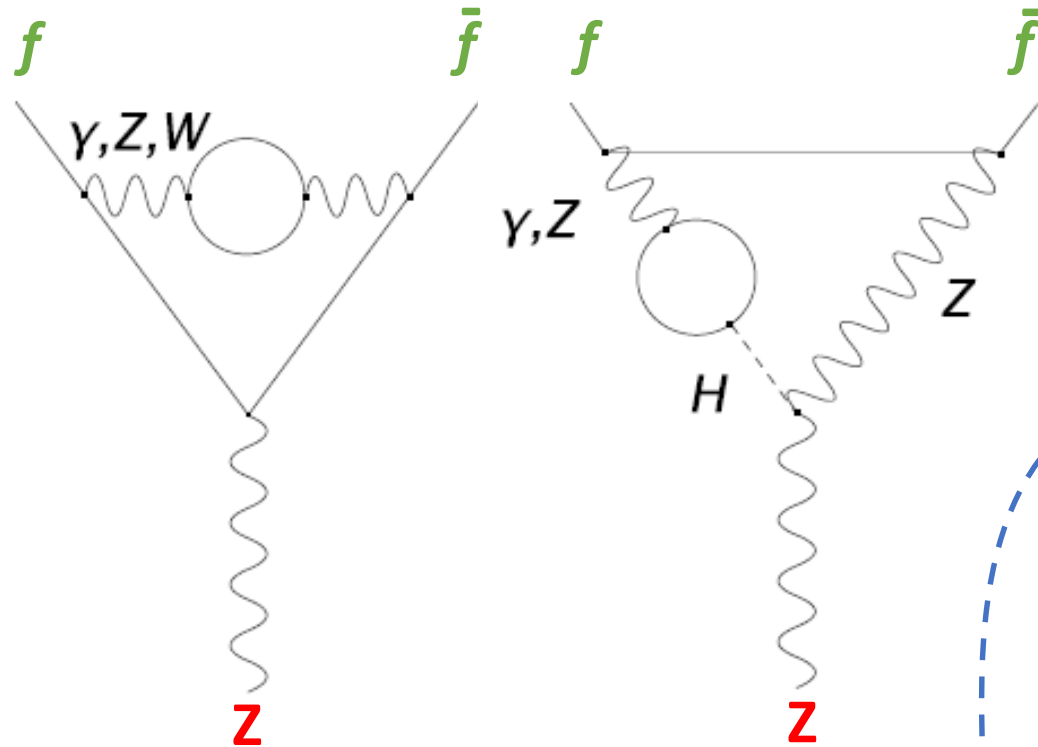
$$\rho_f = 1 + \Delta\rho_{\text{se}} + \dots$$

$$\kappa_f = 1 + \Delta\kappa_{\text{se}} + \dots$$

Z boson couplings to fermions. **Partial widths**, **asymmetries** and the weak mixing angle

A window into the Higgs sector

Loop effects on gauge boson properties



L.O.:

$$g_V^{\text{tree}} \equiv (T_3^f - 2Q_f \sin^2 \theta_W^{\text{tree}})$$

$$g_A^{\text{tree}} \equiv T_3^f.$$



H.O.:

$$g_{Vf} \equiv \sqrt{\rho_f} (T_3^f - 2Q_f \sin^2 \theta_{\text{eff}}^f)$$

$$g_{Af} \equiv \sqrt{\rho_f} T_3^f,$$

$$\sin^2 \theta_{\text{eff}}^f \equiv \kappa_f \sin^2 \theta_W = \kappa_f (1 - m_W^2/m_Z^2)$$

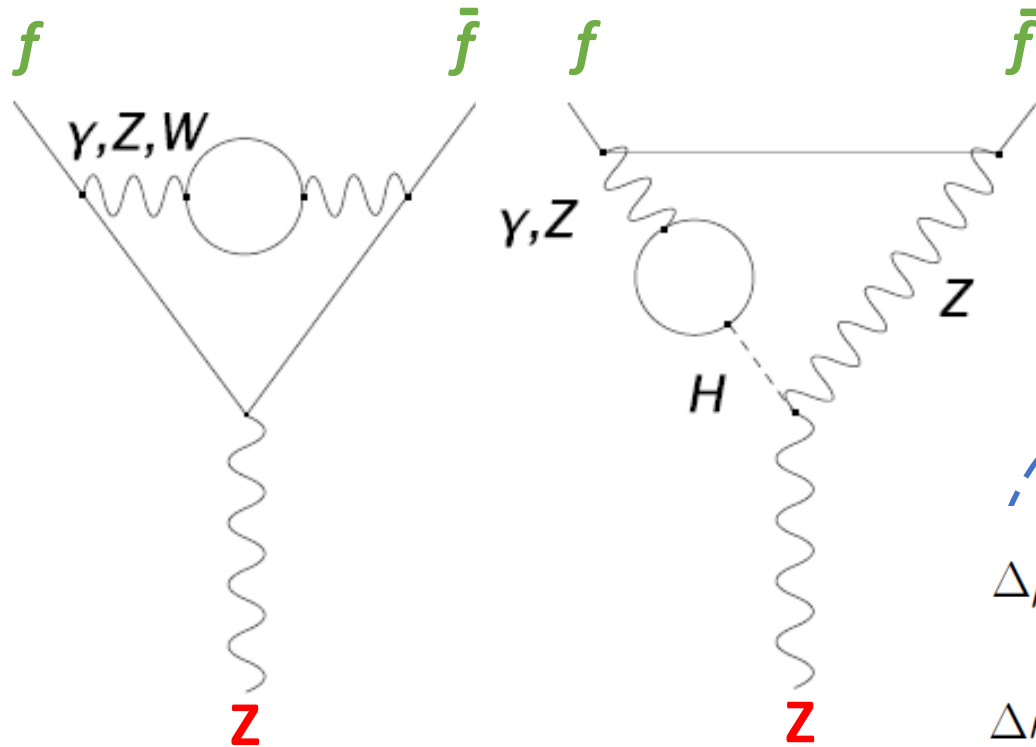
$$\rho_f = 1 + \Delta\rho_{\text{se}} + \dots$$

$$\kappa_f = 1 + \Delta\kappa_{\text{se}} + \dots$$

Z boson couplings to fermions. **Partial widths**, **asymmetries** and the weak mixing angle

A window into the Higgs sector

Loop effects on gauge boson properties



L.O.:

$$g_V^{\text{tree}} \equiv (T_3^f - 2Q_f \sin^2 \theta_W^{\text{tree}})$$

$$g_A^{\text{tree}} \equiv T_3^f.$$



H.O.:

$$g_{Vf} \equiv \sqrt{\rho_f} (T_3^f - 2Q_f \sin^2 \theta_{\text{eff}}^f)$$

$$g_{Af} \equiv \sqrt{\rho_f} T_3^f,$$

$$\sin^2 \theta_{\text{eff}}^f \equiv \kappa_f \sin^2 \theta_W = \kappa_f (1 - m_W^2/m_Z^2)$$

$$\rho_f = 1 + \Delta\rho_{\text{se}} + \dots$$

$$\kappa_f = 1 + \Delta\kappa_{\text{se}} + \dots$$

$$\Delta\rho_{\text{se}} = \frac{3G_F m_W^2}{8\sqrt{2}\pi^2} \left[\frac{m_t^2}{m_W^2} \frac{\sin^2 \theta_W}{\cos^2 \theta_W} \left(\ln \frac{m_H^2}{m_W^2} - \frac{5}{6} \right) + \dots \right]$$

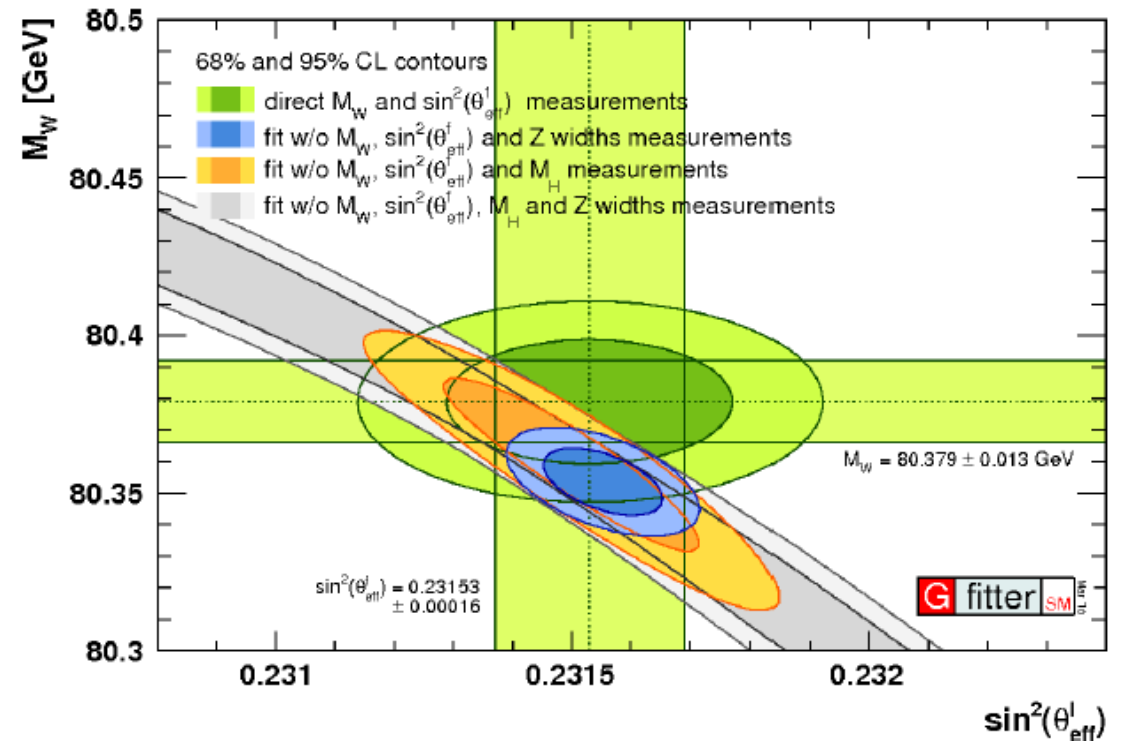
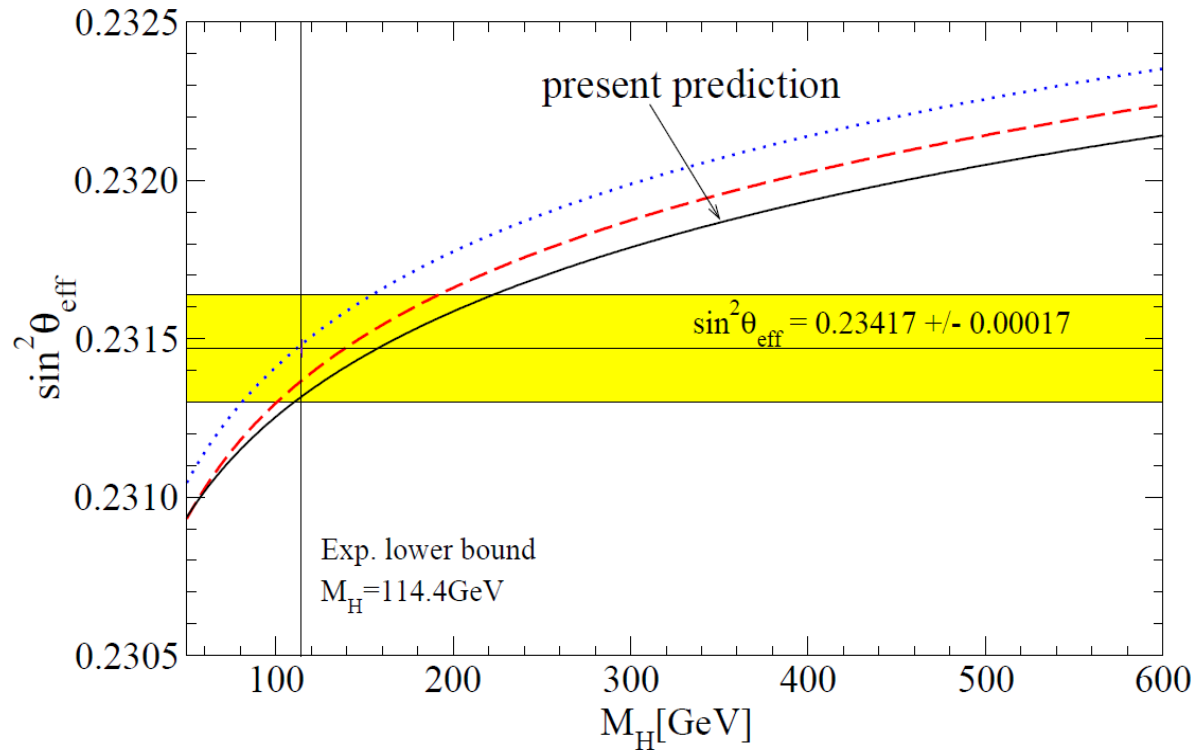
$$\Delta\kappa_{\text{se}} = \frac{3G_F m_W^2}{8\sqrt{2}\pi^2} \left[\frac{m_t^2 \cos^2 \theta_W}{m_W^2 \sin^2 \theta_W} - \frac{10}{9} \left(\ln \frac{m_H^2}{m_W^2} - \frac{5}{6} \right) + \dots \right]$$



Z boson couplings to fermions. **Partial widths**, **asymmetries** and the weak mixing angle

A window into the Higgs sector

Loop effects on gauge boson properties



Z boson couplings to fermions. Partial widths, asymmetries and the weak mixing angle

A window into the Higgs sector

Loop effects on gauge boson properties : the W boson mass

At leading order, m_W is expressed as

$$m_W^2 \sin^2 \theta_W = \frac{\pi \alpha}{\sqrt{2} G_\mu}, \quad \sin^2 \theta_W = 1 - m_W^2 / m_Z^2$$

Higher-order corrections, dominantly W and γ self-energies,

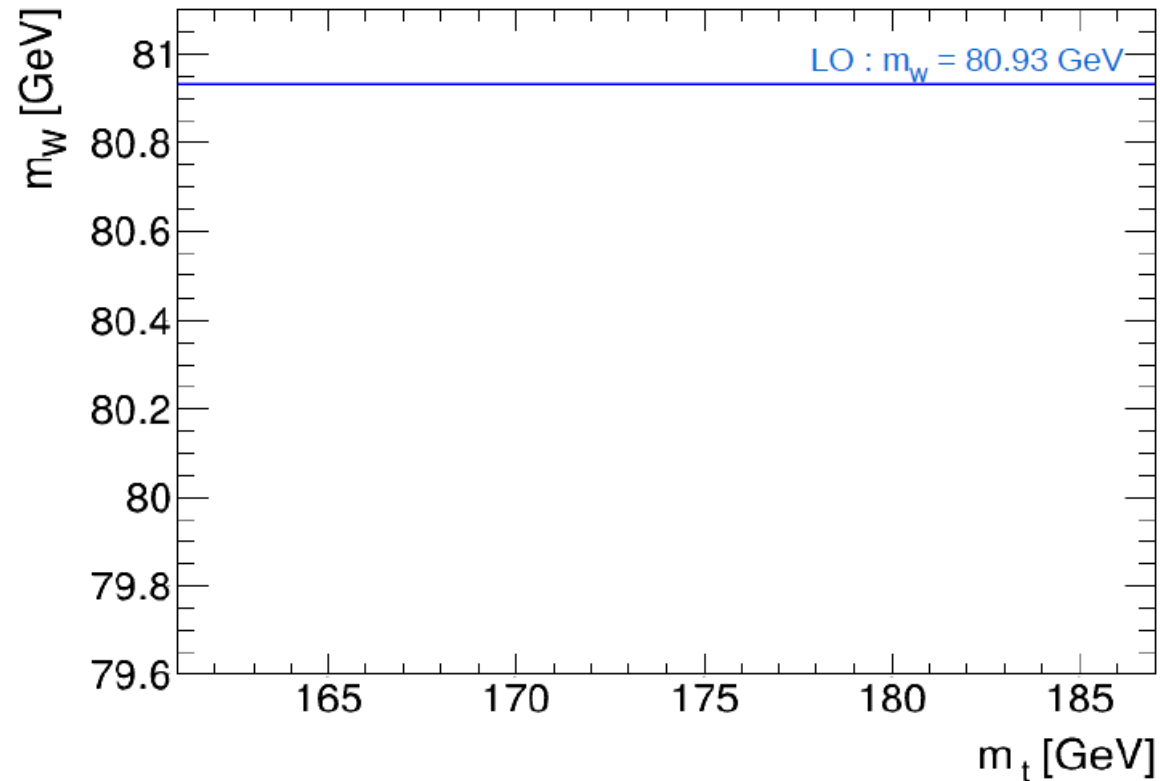


modify this relation to
$$m_W^2 \sin^2 \theta_W = \frac{\pi \alpha}{\sqrt{2} G_\mu} \frac{1}{1 - \Delta r}$$

A window into the Higgs sector

Loop effects on gauge boson properties : the W boson mass

$$\Delta r = 0 \quad (\text{leading order})$$

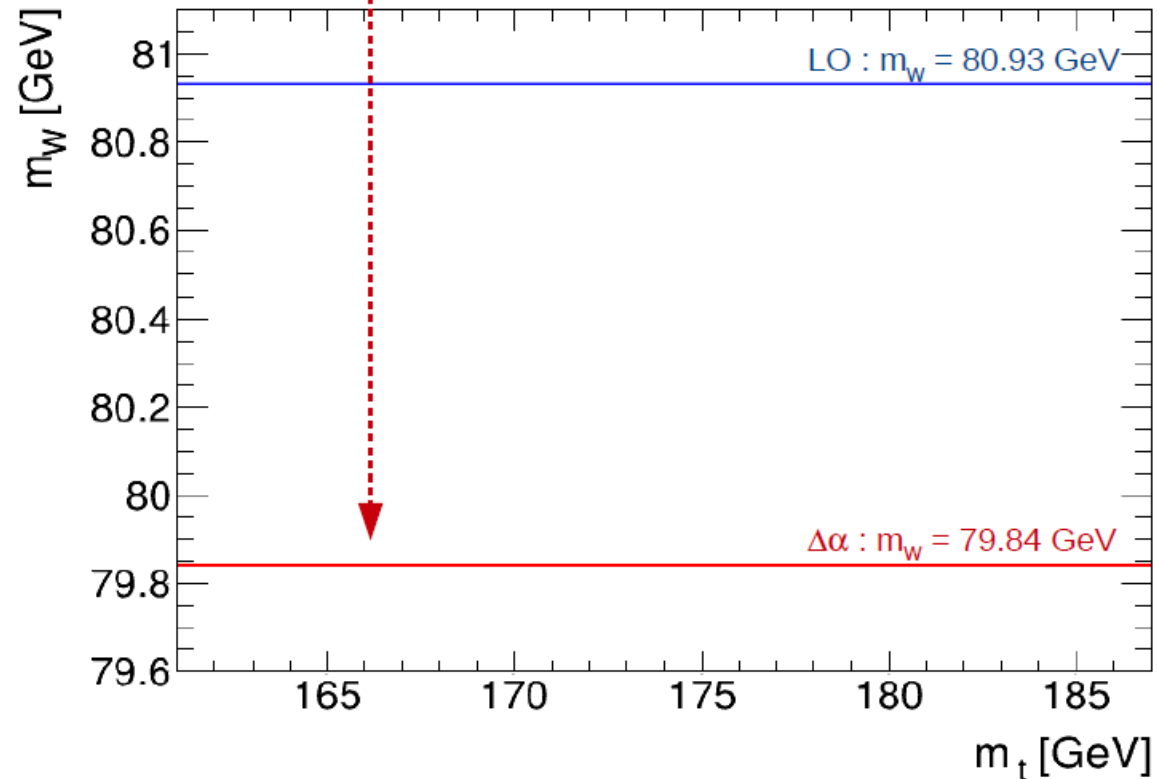


A window into the Higgs sector

Loop effects on gauge boson properties : the W boson mass

$$\Delta r = \Delta \alpha$$

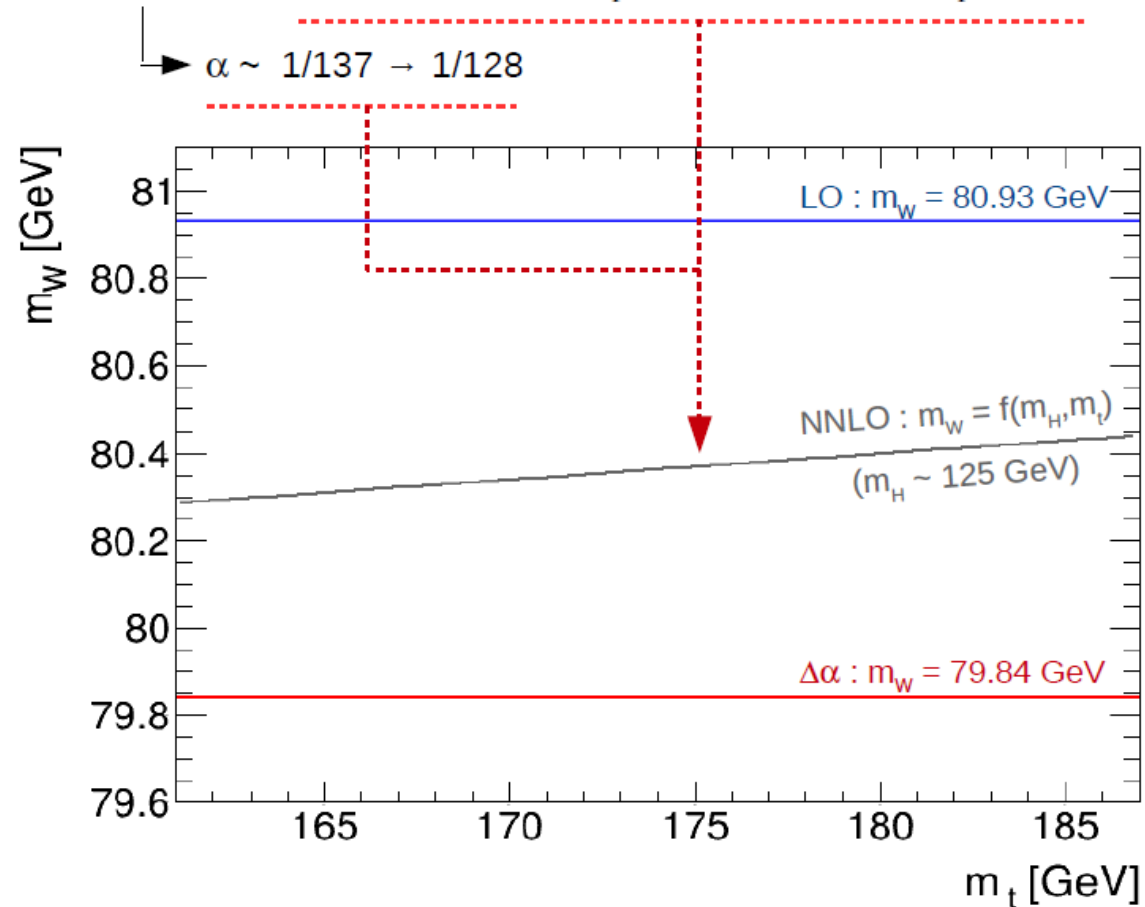
$\alpha \sim 1/137 \rightarrow 1/128$



A window into the Higgs sector

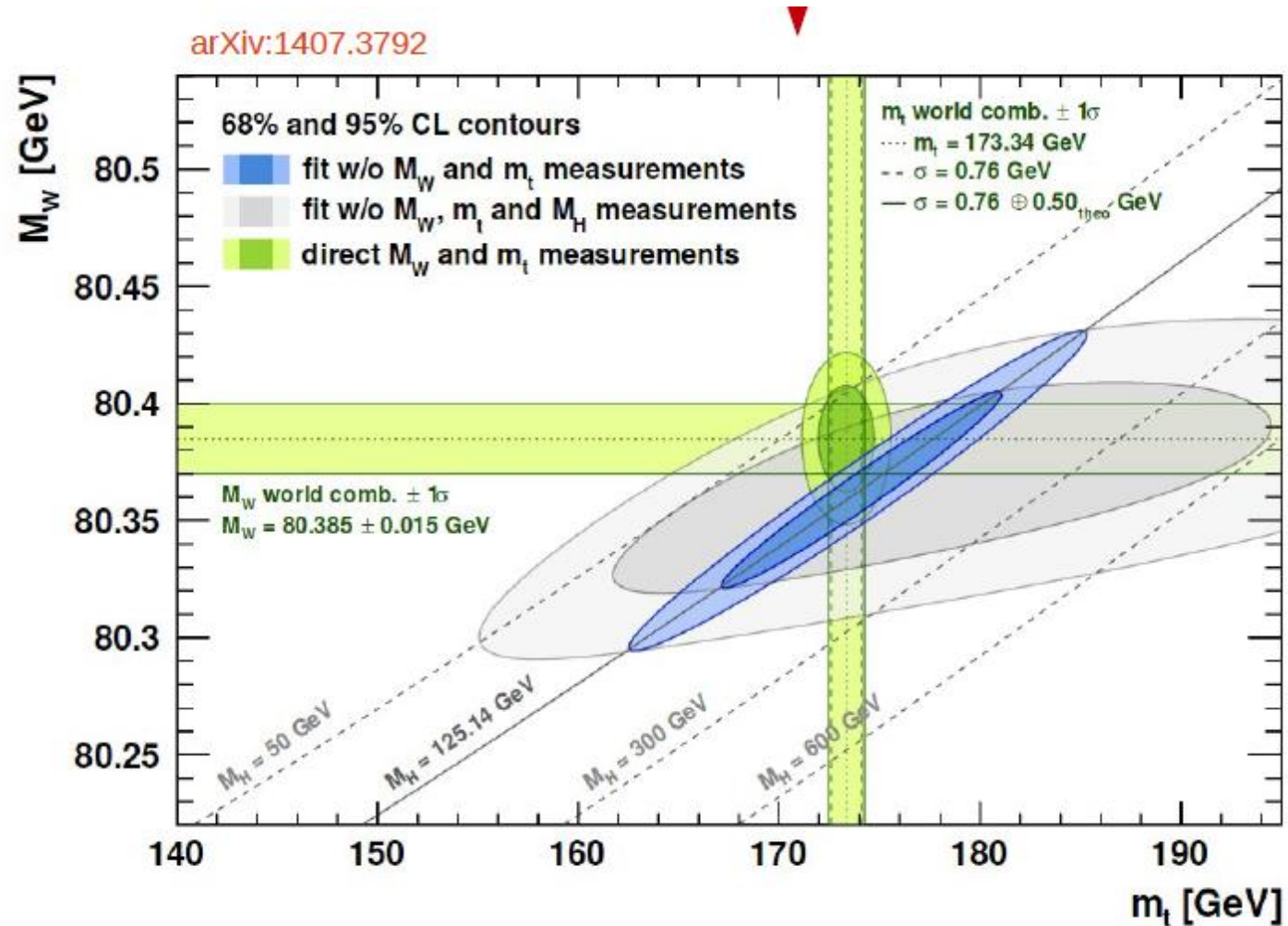
Loop effects on gauge boson properties : the W boson mass

$$\Delta r = \Delta\alpha - \tan\theta_W \Delta\rho(m_{top}) + \Delta r_{rem}^{SM}(m_{top}, m_H) + \dots$$



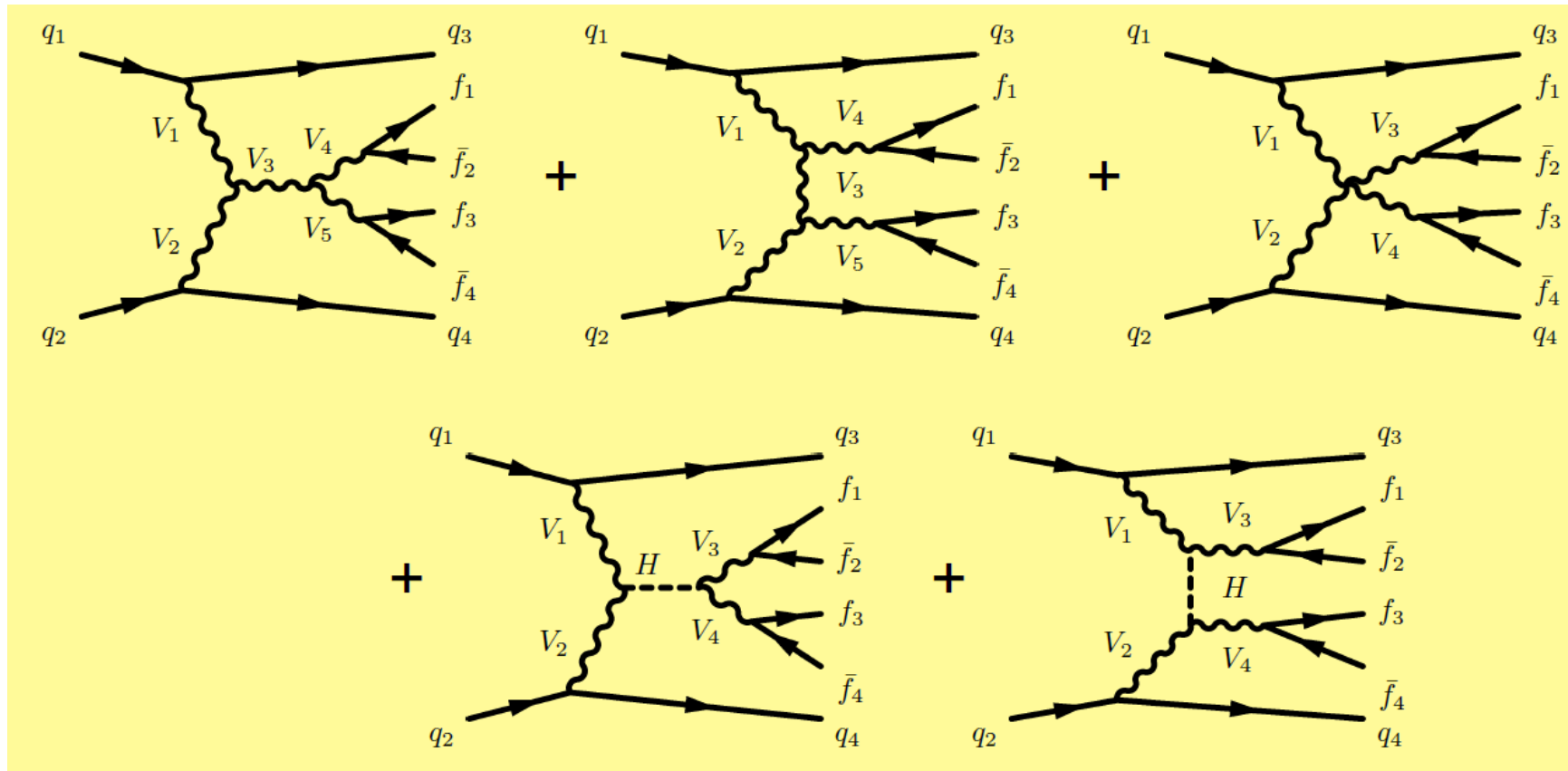
A window into the Higgs sector

Loop effects on gauge boson properties : the W boson mass



A window into the Higgs sector

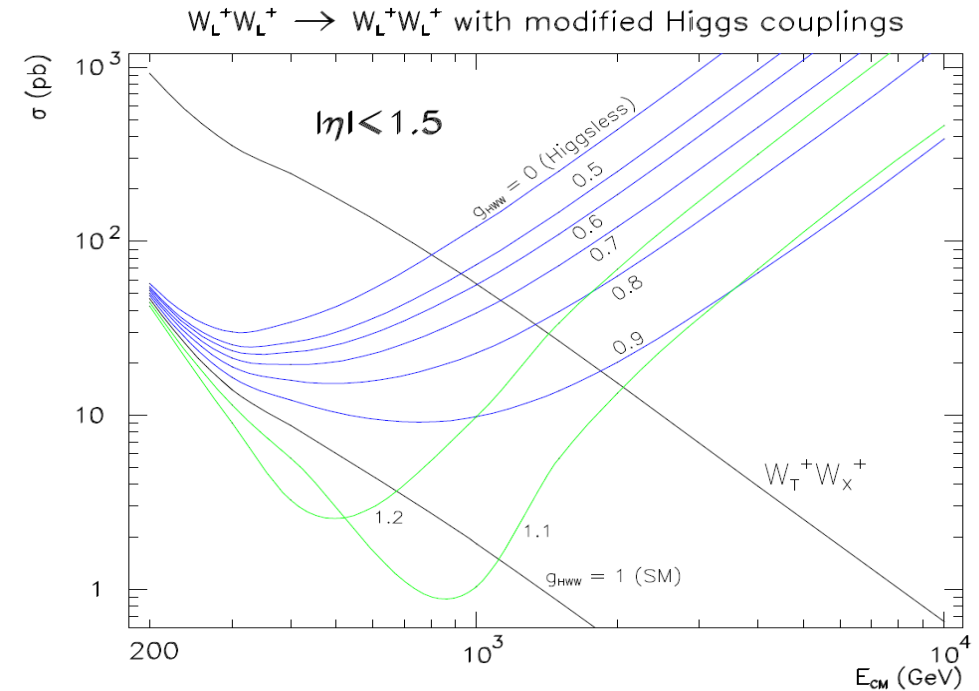
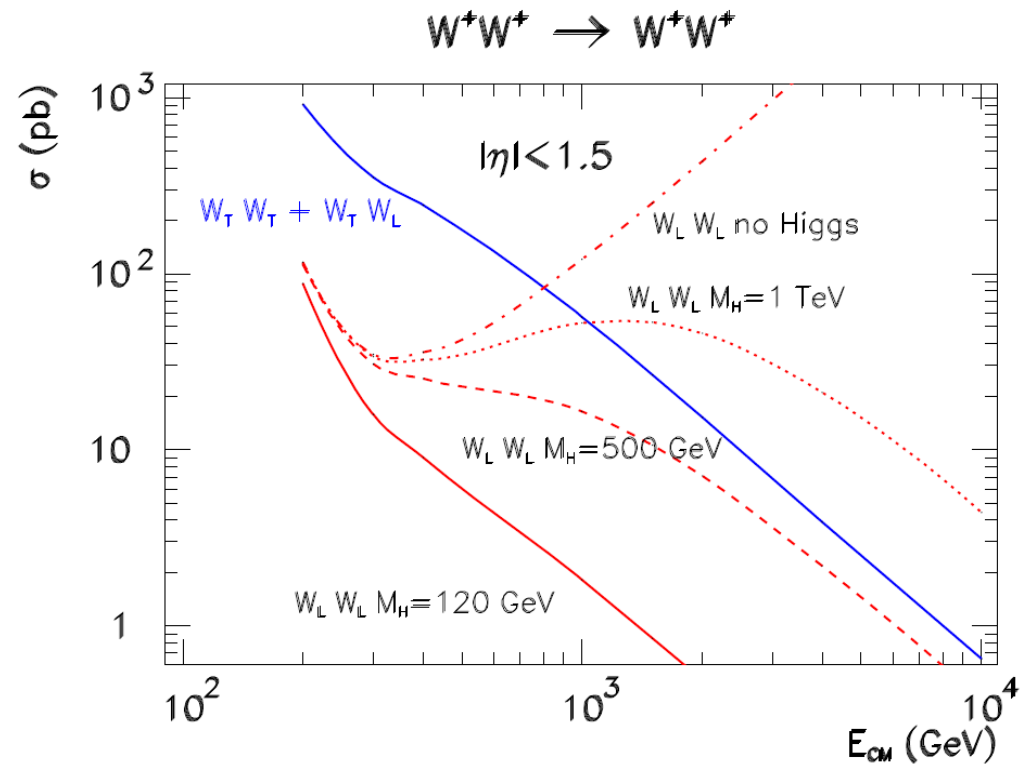
Real contributions to weak boson interactions



Vector boson scattering at high energy

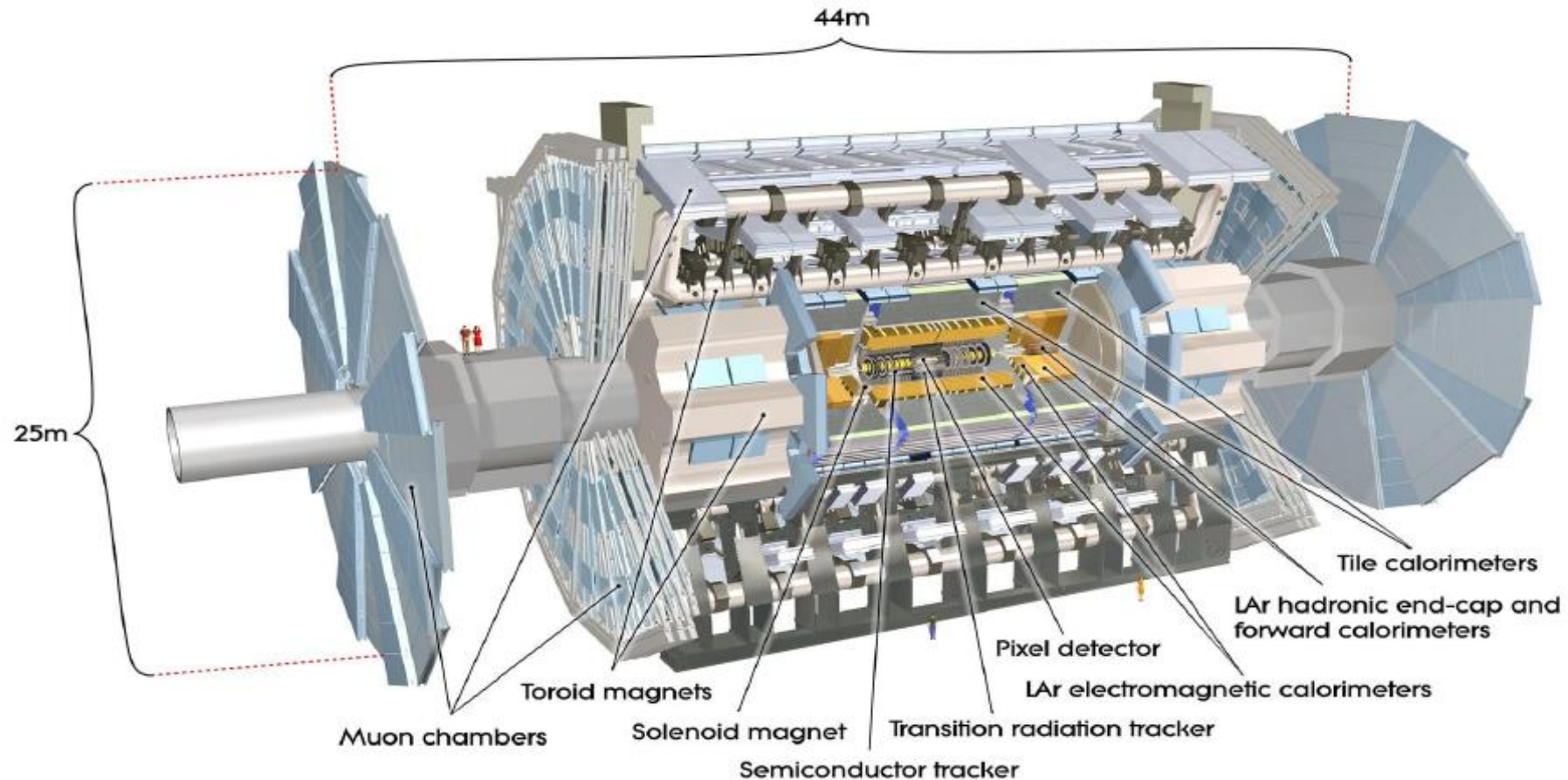
A window into the Higgs sector

Real contributions to weak boson interactions



Vector boson scattering at high energy

The ATLAS detector



Of particular importance to the measurements discussed here :

Muons (Inner Detector, Muon Spectrometer)

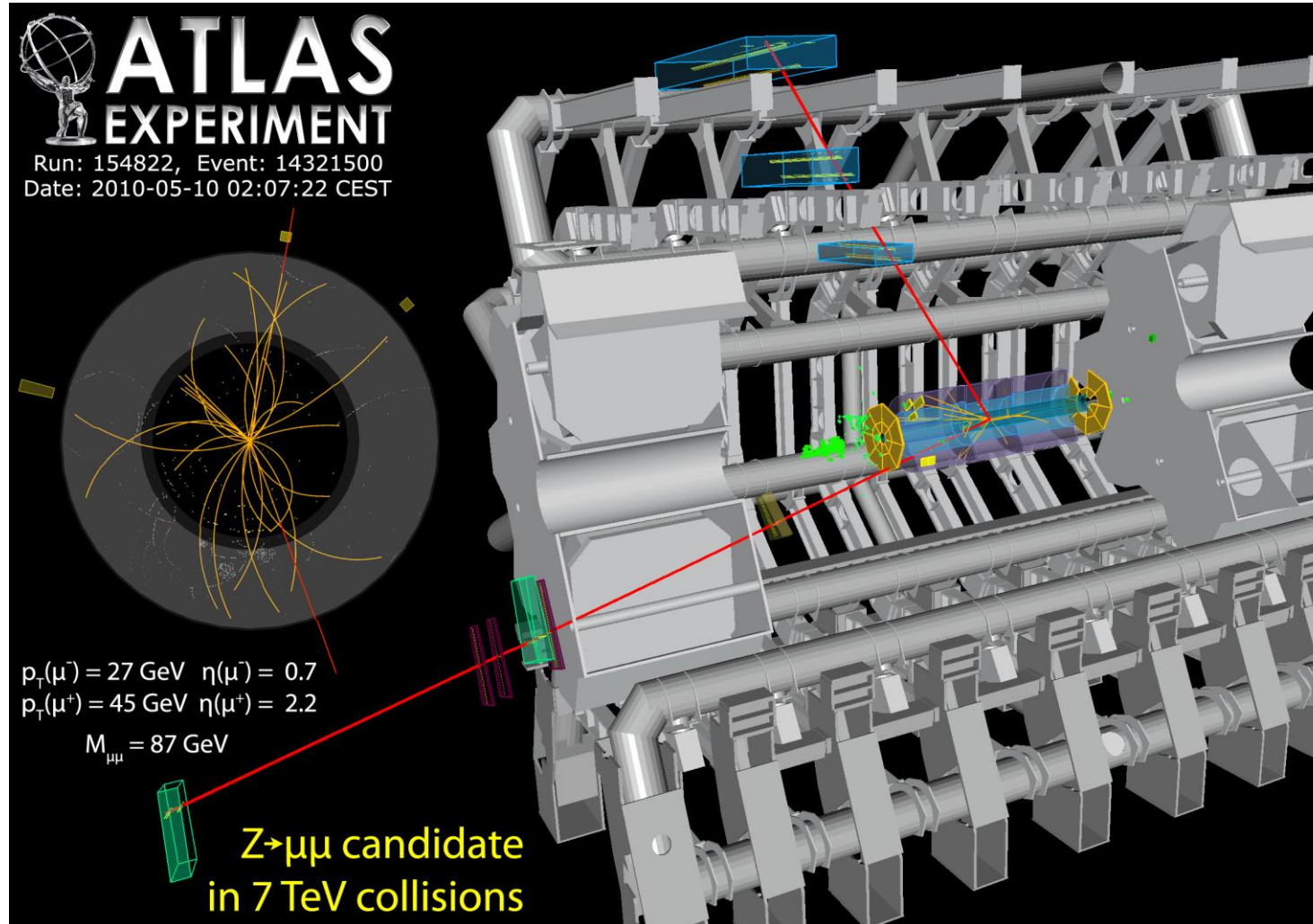
Electrons (Inner Detector, EM calorimeter & forward calorimeters)

Missing transverse energy (full calorimeter system)

The effective weak mixing angle

$$pp \rightarrow \ell^+ \ell^- + X$$

An example Z candidate



Effective mixing angle from the lepton angular distributions

Factorized expression for Z boson production and decay at hadron colliders:

$$\frac{d^5\sigma}{dp_T^Z dy^Z dm^Z d\cos\theta d\phi}$$

$$= \frac{3}{16\pi} \frac{d^3\sigma^{U+L}}{dp_T^Z dy^Z dm^Z}$$

Production

Decay

$$\{(1 + \cos^2\theta) + 1/2 A_0(1 - 3\cos^2\theta) + A_1 \sin 2\theta \cos\phi + 1/2 A_2 \sin^2\theta \cos 2\phi + A_3 \sin\theta \cos\phi + A_4 \cos\theta + A_5 \sin^2\theta \sin 2\phi + A_6 \sin 2\theta \sin\phi + A_7 \sin\theta \sin\phi\}.$$

Effective mixing angle from the lepton angular distributions

Factorized expression for Z boson production and decay at hadron colliders:

$$\frac{d^5\sigma}{dp_T^Z dy^Z dm^Z d\cos\theta d\phi}$$

$$= \frac{3}{16\pi} \frac{d^3\sigma^{U+L}}{dp_T^Z dy^Z dm^Z}$$

Production

Decay

$$\{(1 + \cos^2 \theta) + 1/2 A_0(1 - 3 \cos^2 \theta) + A_1 \sin 2\theta \cos \phi + 1/2 A_2 \sin^2 \theta \cos 2\phi + A_3 \sin \theta \cos \phi + A_4 \cos \theta + A_5 \sin^2 \theta \sin 2\phi + A_6 \sin 2\theta \sin \phi + A_7 \sin \theta \sin \phi\}.$$

Unpolarized cross section

Effective mixing angle from the lepton angular distributions

Factorized expression for Z boson production and decay at hadron colliders:

$$\frac{d^5\sigma}{dp_T^Z dy^Z dm^Z d\cos\theta d\phi}$$

$$= \frac{3}{16\pi} \frac{d^3\sigma^{U+L}}{dp_T^Z dy^Z dm^Z}$$

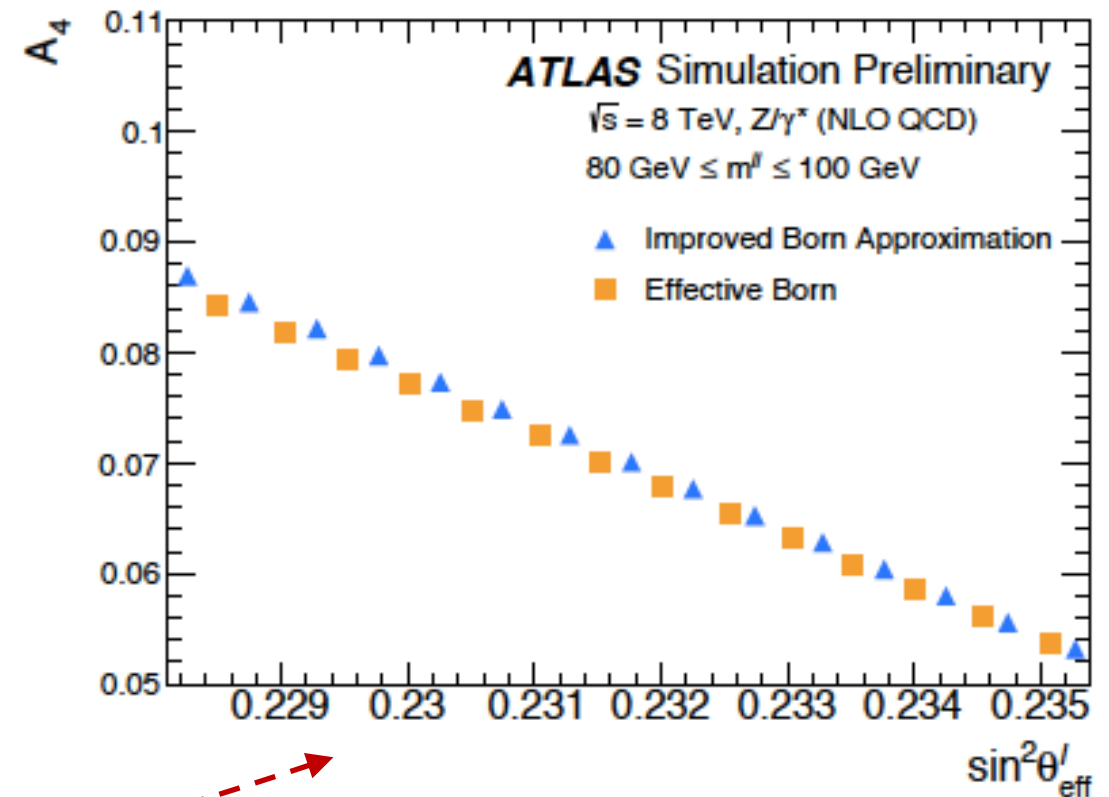
Production
Decay

$$\{(1 + \cos^2\theta) + 1/2 A_0(1 - 3\cos^2\theta) + A_1 \sin 2\theta \cos\phi + 1/2 A_2 \sin^2\theta \cos 2\phi + A_3 \sin\theta \cos\phi + A_4 \cos\theta + A_5 \sin^2\theta \sin 2\phi + A_6 \sin 2\theta \sin\phi + A_7 \sin\theta \sin\phi\}.$$

Unpolarized cross section

F/B asymmetry :

$$A_4 = 8/3 A_{\text{FB}} \sim a + b \sin^2\theta_{\text{eff}}^l$$



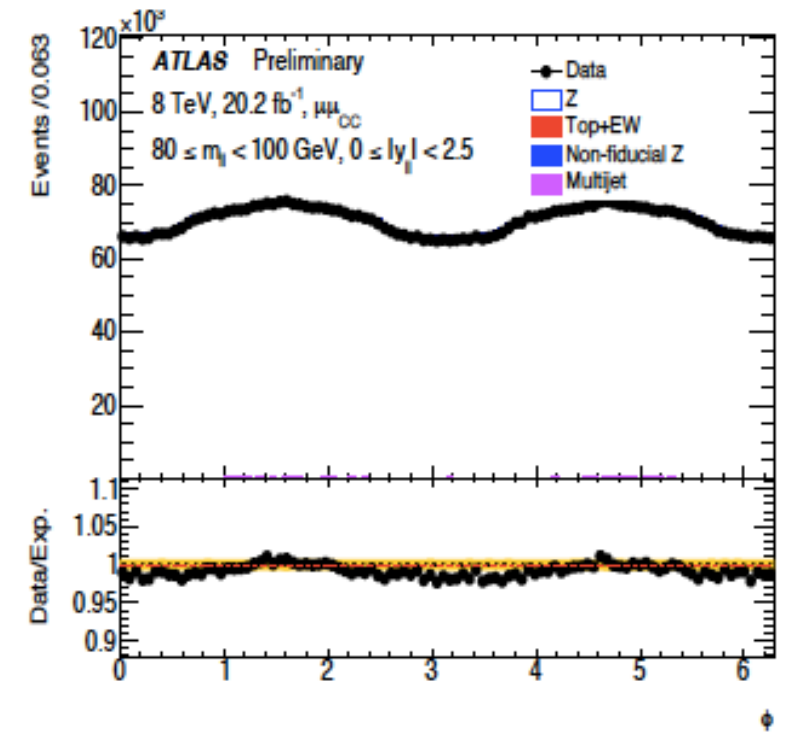
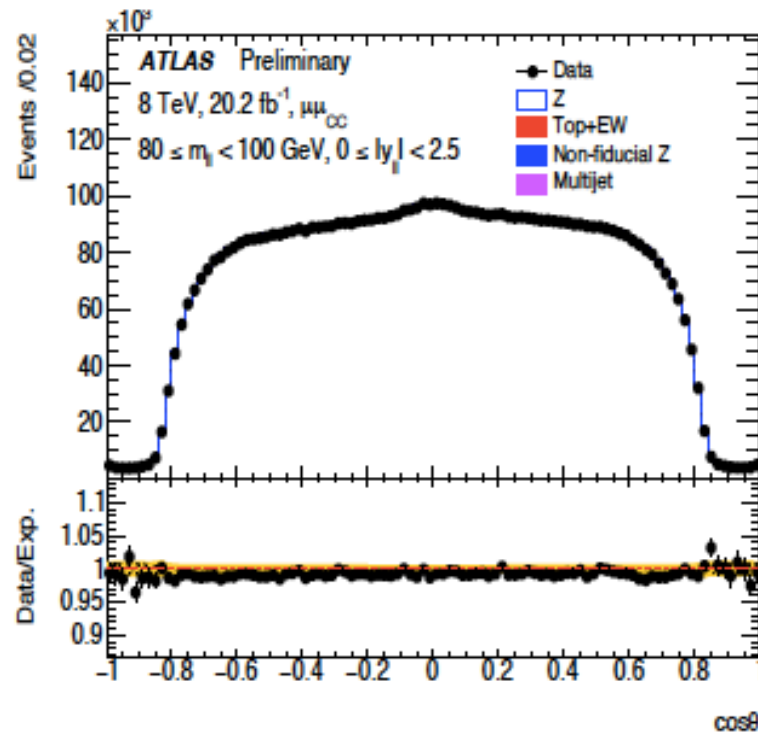
Measurement of the A_i coefficients (20 fb⁻¹, 8 TeV)

The observed angular distributions reflect the angular decomposition discussed above:

Event selection :

- Two muons of opposite charge
- $p_T > 20$ GeV
- $|\eta| < 2.5$

8M candidates in the muon channel.
Similar selections in the electron channel.



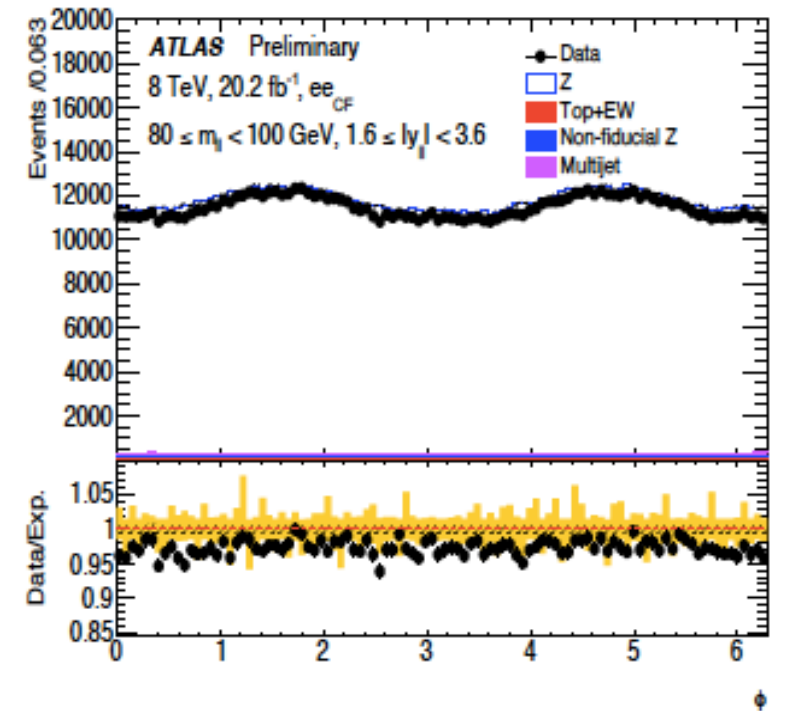
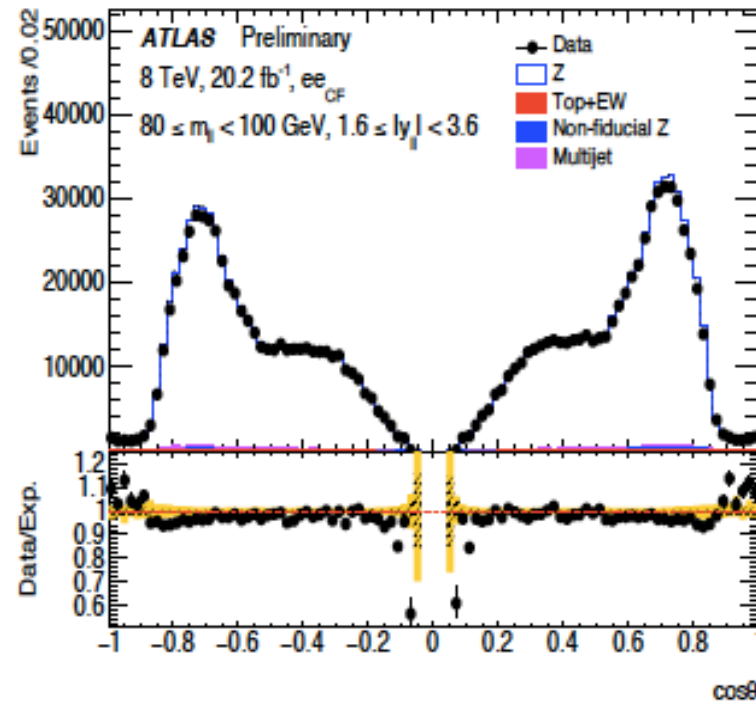
Measurement of the A_i coefficients

The observed angular distributions reflect the angular decomposition discussed above:

Event selection :

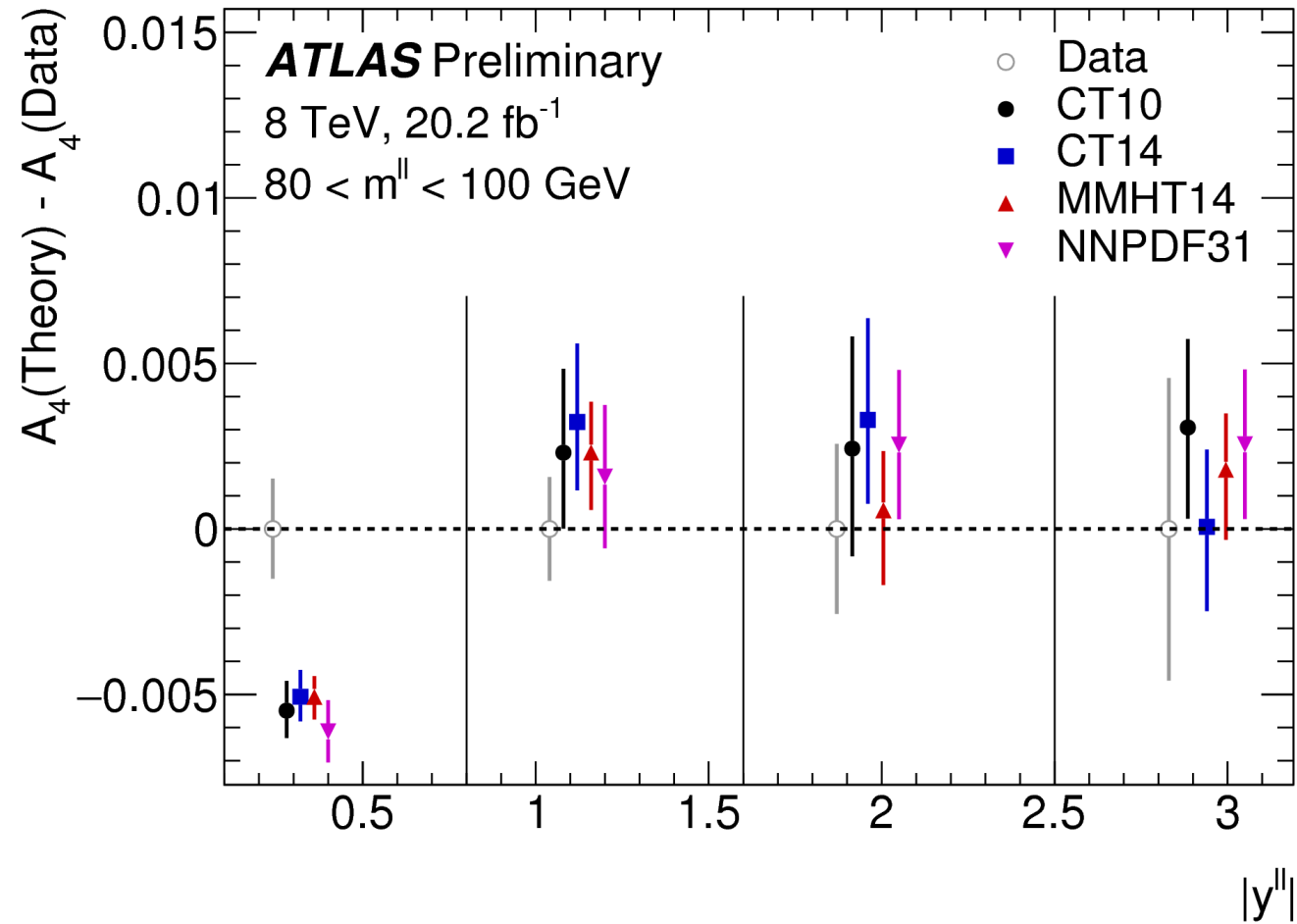
- Two reconstructed electrons
- $p_T > 20$ GeV
- $|\eta_1| < 2.5, 2.5 < |\eta_2| < 4.9$

1.1M candidates from 20 fb^{-1} at 8 TeV



Measurement of the A_i coefficients

Results:

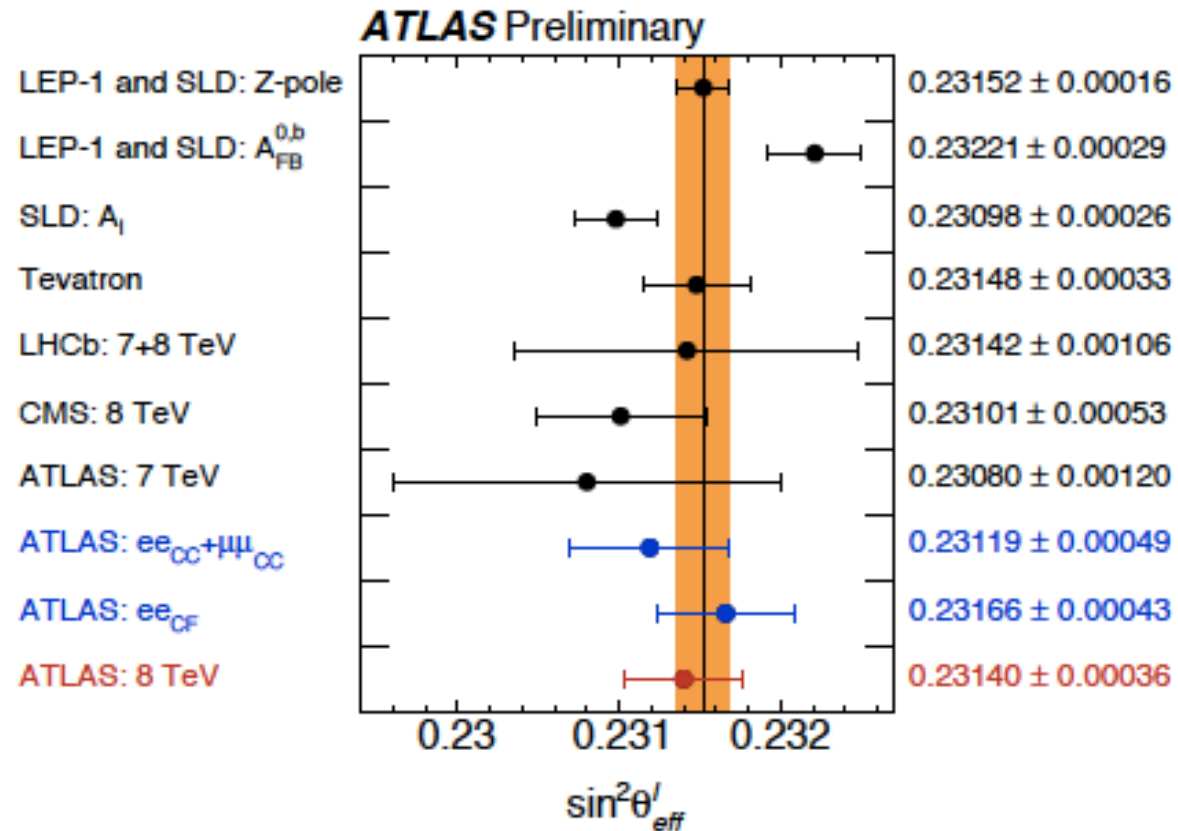


Predictions include PDF uncertainties for the four different PDF sets, And assume $\sin^2\theta_W = 0.23152$.

Electrons and muons contribute for $|y| < 2.5$, Only electrons contribute for $|y| > 2.5$.

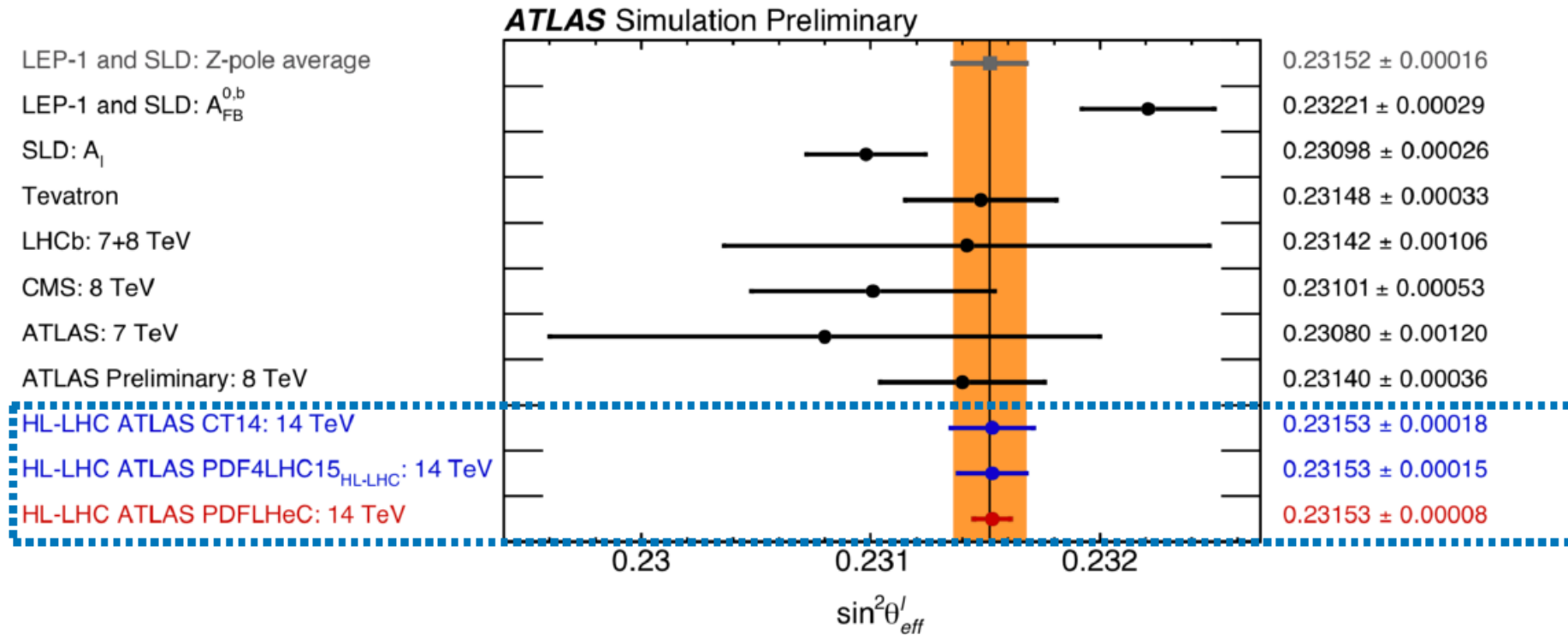
Results for the effective weak mixing angle

$$\sin^2\theta_{\text{eff}}^l = 0.23140 \pm 0.00021 \text{ (stat.)} \pm 0.00024 \text{ (PDF)} \pm 0.00016 \text{ (syst.)}$$



Competitive in precision with the previous best individual measurements (world average still a factor two better).

Prospects at the HL-LHC



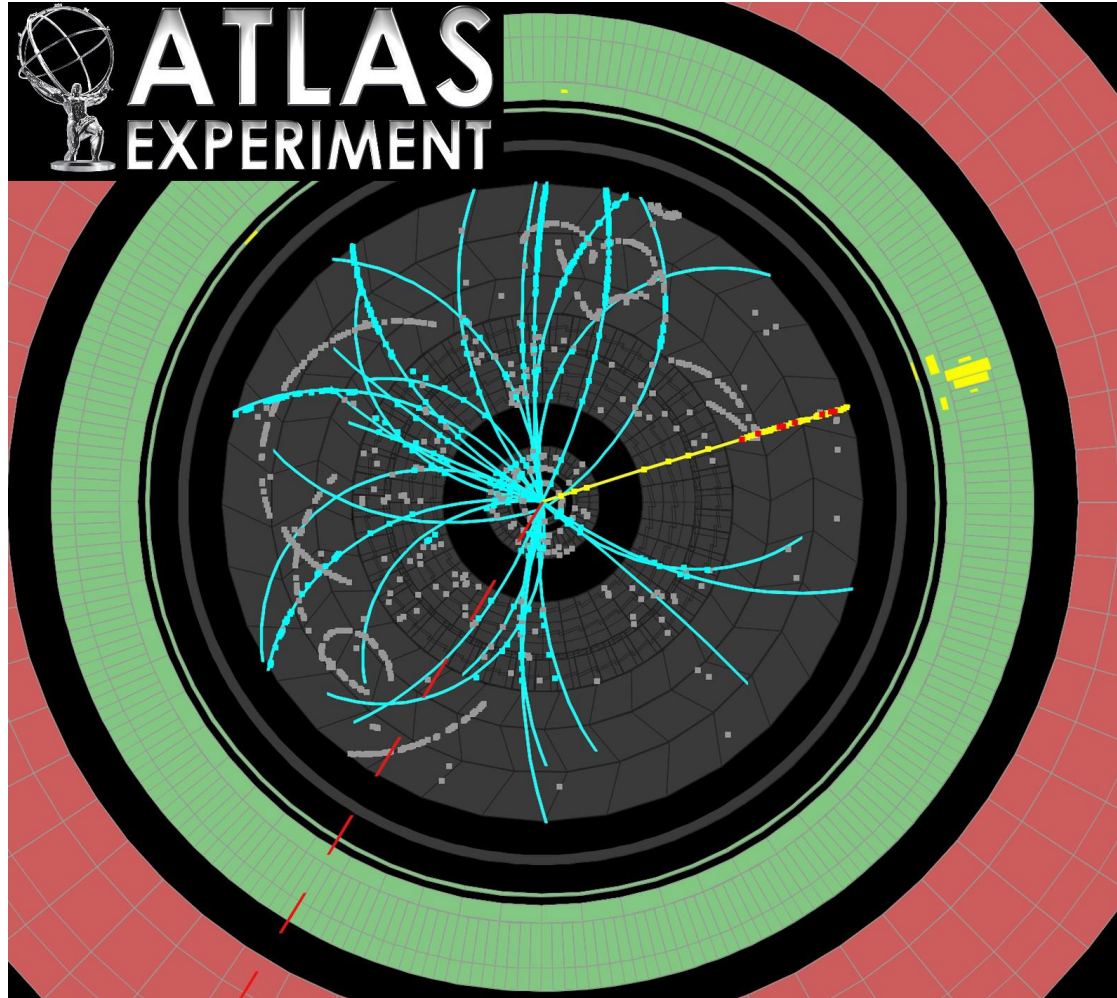
Prospects @HL-LHC:

- reduction of statistical uncertainty (3000 fb^{-1})
 - Extended pseudo-rapidity coverage ($|\eta| < 4$)
 - Expected reduction of PDF uncertainties
- Including LHeC data: reduction of PDF (total) uncertainties by a factor of ~ 5 (2) wrt to HL-LHC PDFs.

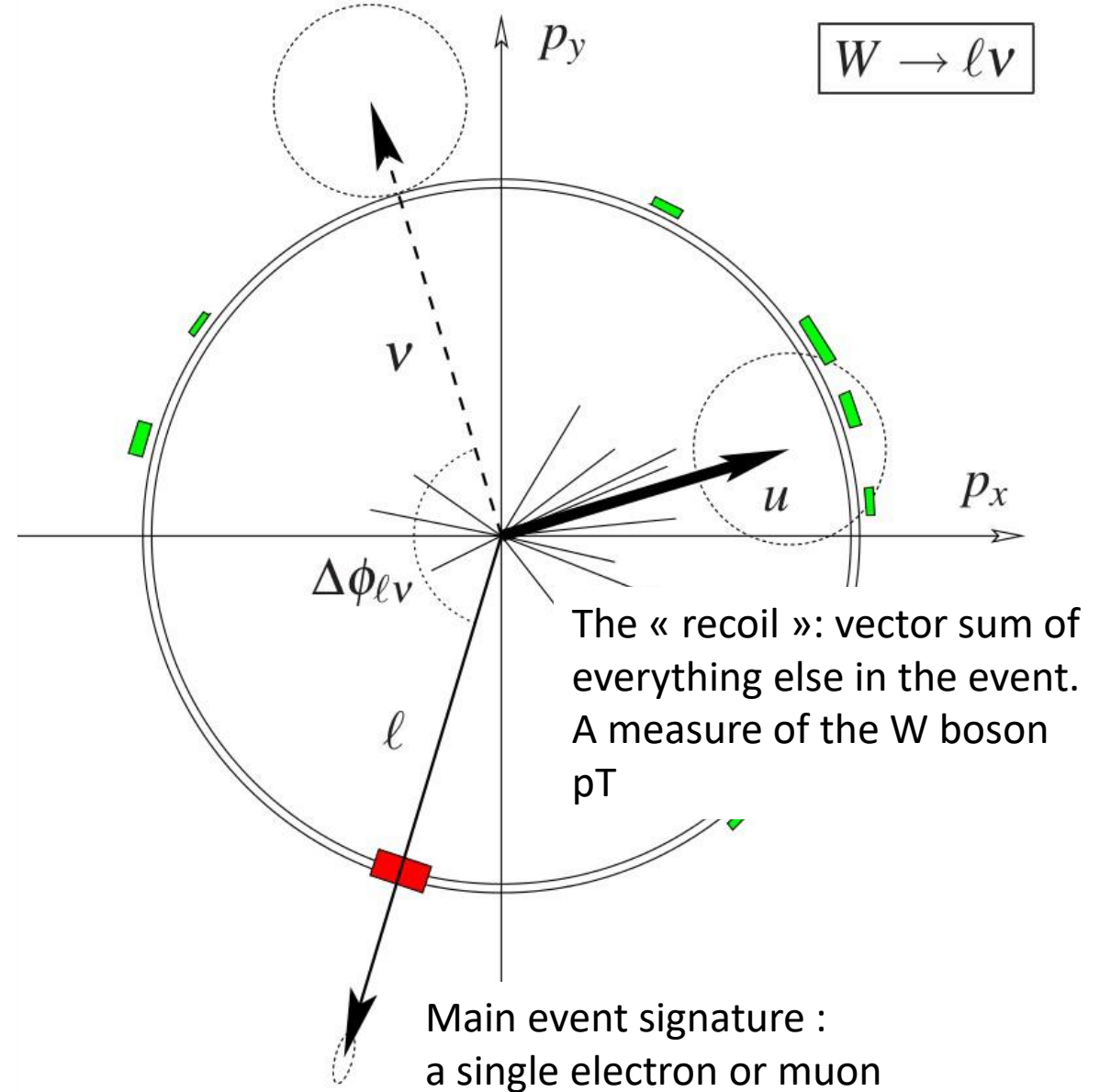
The W boson mass

$$pp \rightarrow \ell^\pm \nu + X$$

Event representation



Derived quantities : missing transverse energy (measures the neutrino p_T); transverse mass



Measurement setup (5 fb⁻¹, 7 TeV)

Lepton selections

- Muons : $|\eta| < 2.4$; isolated (track-based)
- Electrons : $0 < |\eta| < 1.2$ or $1.8 < |\eta| < 2.4$; isolated (track+calorimeter-based)

Kinematic requirements

- $p_T^l > 30$ GeV $p_T^{\text{miss}} > 30$ GeV
- $m_T > 60$ GeV $u_T < 30$ GeV

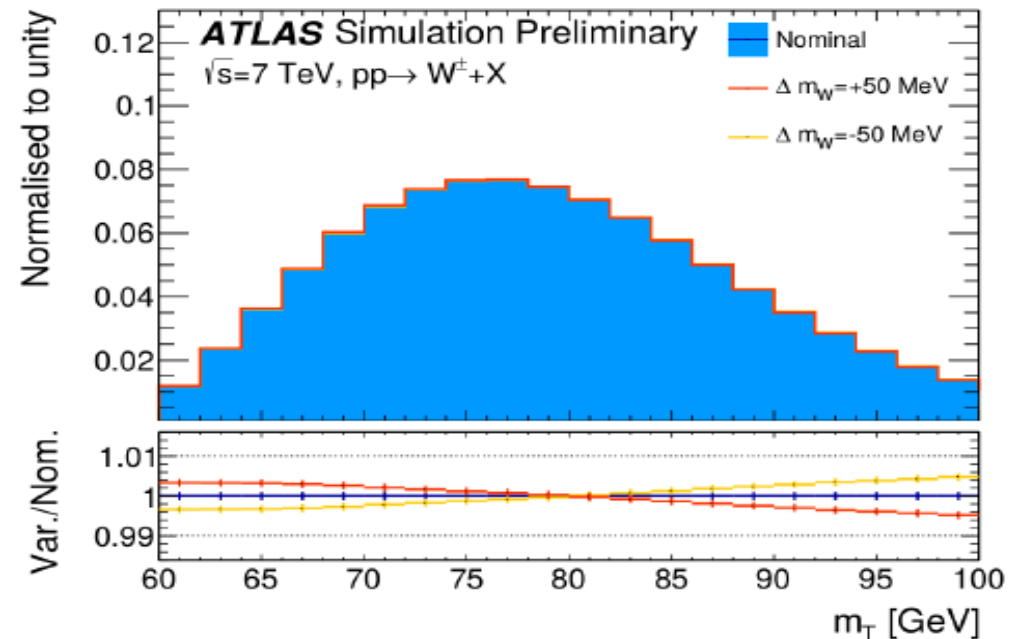
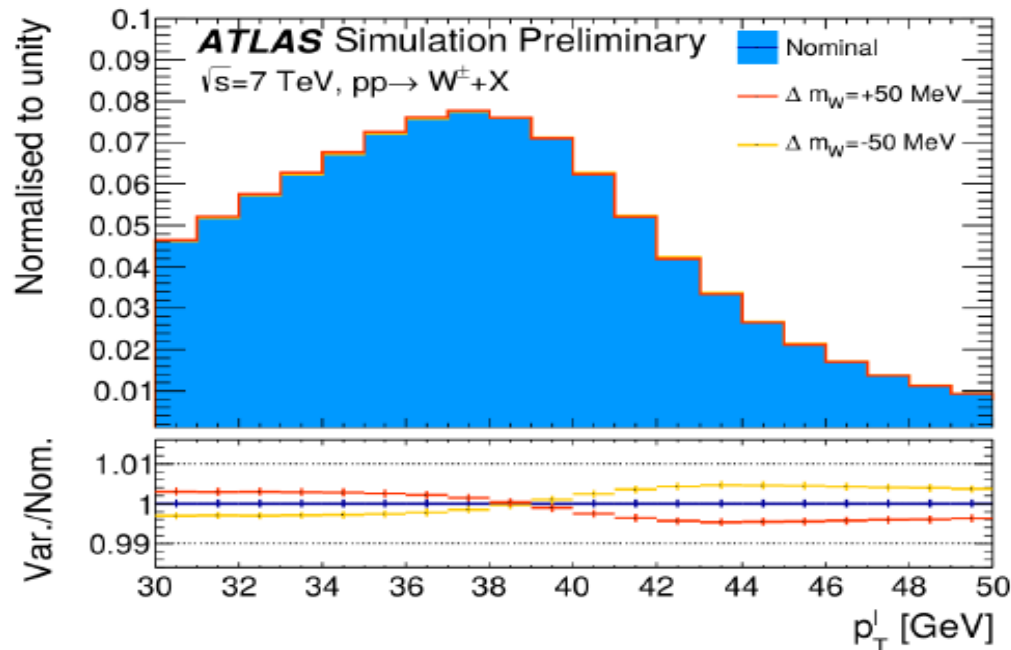
Measurement categories :

$ \eta_\ell $ range	0 – 0.8	0.8 – 1.4	1.4 – 2.0	2.0 – 2.4	Inclusive	
$W^+ \rightarrow \mu^+ \nu$	1 283 332	1 063 131	1 377 773	885 582	4 609 818	7.8 M events
$W^- \rightarrow \mu^- \bar{\nu}$	1 001 592	769 876	916 163	547 329	3 234 960	
$ \eta_\ell $ range	0 – 0.6	0.6 – 1.2		1.8 – 2.4	Inclusive	
$W^+ \rightarrow e^+ \nu$	1 233 960	1 207 136		956 620	3 397 716	5.9 M events
$W^- \rightarrow e^- \bar{\nu}$	969 170	908 327		610 028	2 487 525	

Measurement strategy

Mass fits

- Sensitive final state distributions : p_T^l , m_T , p_T^{miss}
- Signal distributions constructed from a single Monte Carlo sample, reweighting the boson invariant mass distribution, and compared to data. Mass determination by χ^2 minimization
- Resonance parametrisation : $\frac{d\sigma}{dm} \propto \frac{m^2}{(m^2 - m_V^2)^2 + m^4 \Gamma_V^2 / m_V^2}$
- A blinding offset was applied throughout the measurement, and removed when consistent results were found (compatibility among decay channels, etc).



Measurement strategy

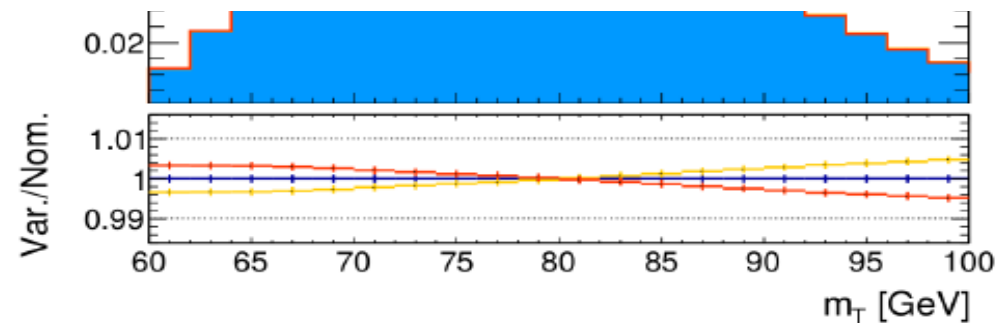
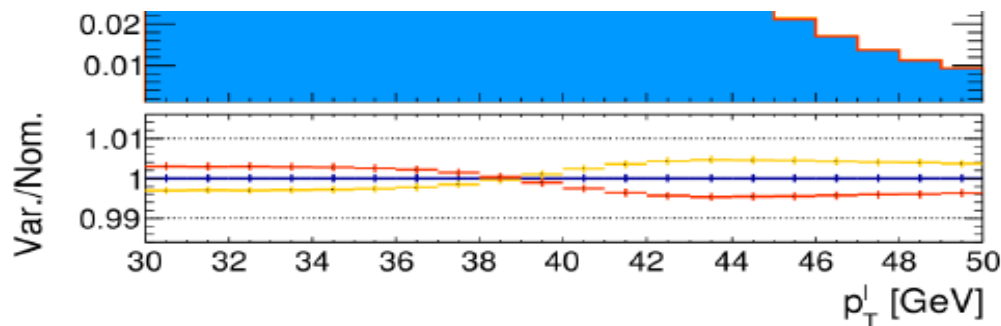
Mass fits

- Sensitive final state distributions : p_T^l , m_T , $p_{T^{\text{miss}}}$
- Signal distributions constructed from a single Monte Carlo sample, reweighting the boson invariant mass distribution and compared to data. Mass determination by χ^2 minimization

Extremely simple in principle, but all effects entering the observed distributions:

- Detector calibration
- Physics modelling of W production and decay

need to be controlled to **0.01 – 0.1%**



Timeline (main project and ancillary measurements)

2011

2012

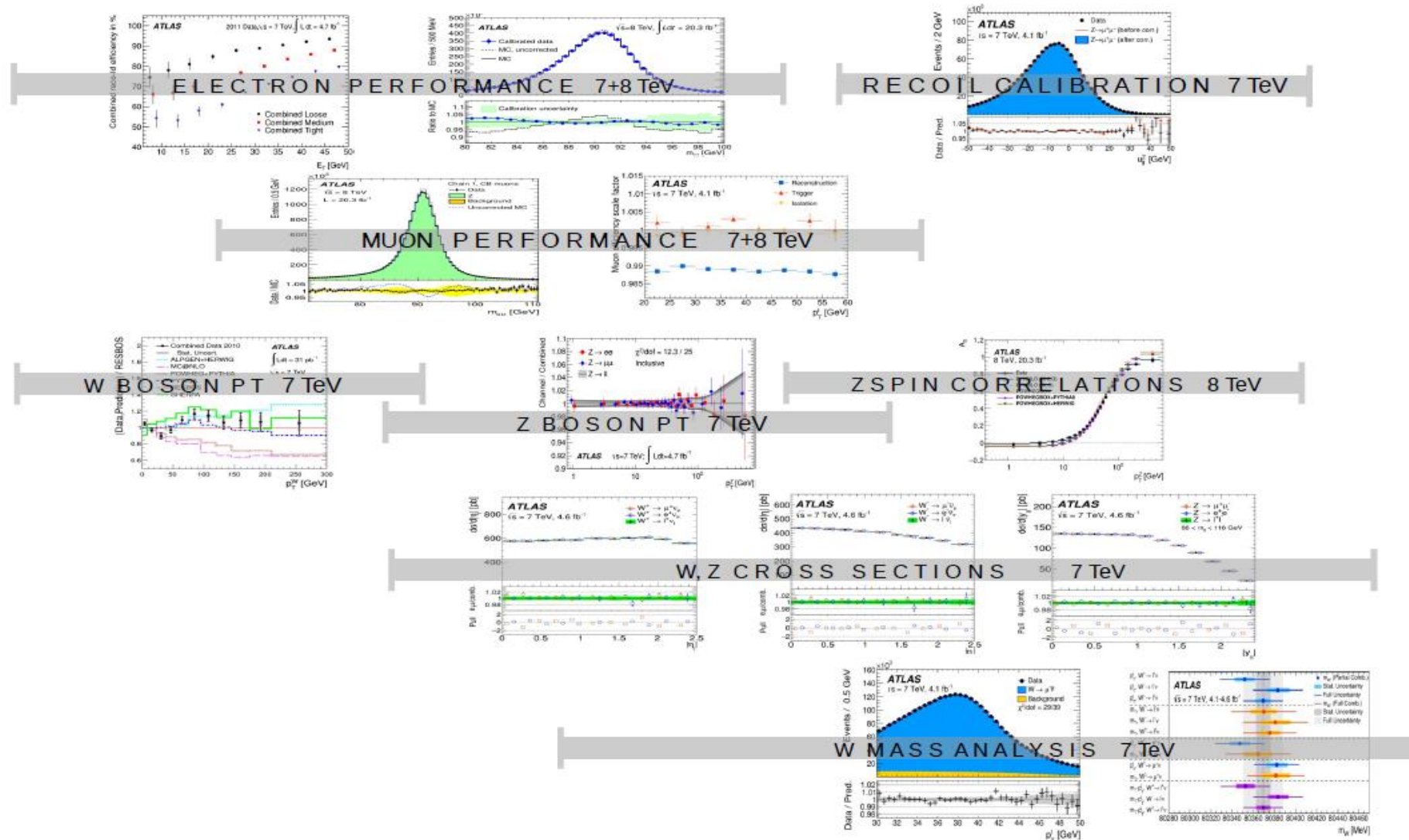
2013

2014

2015

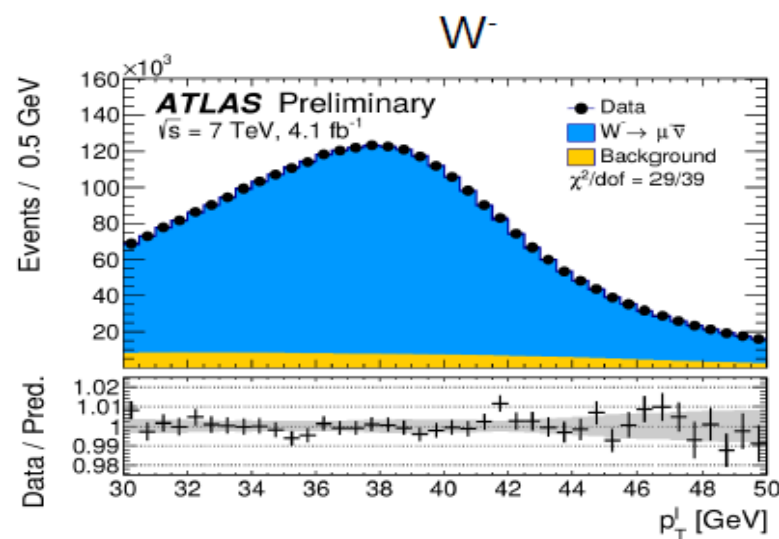
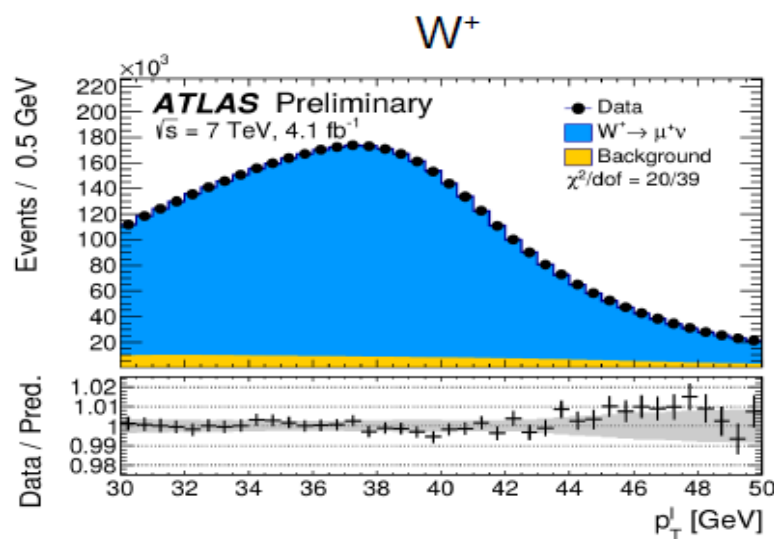
2016

2017

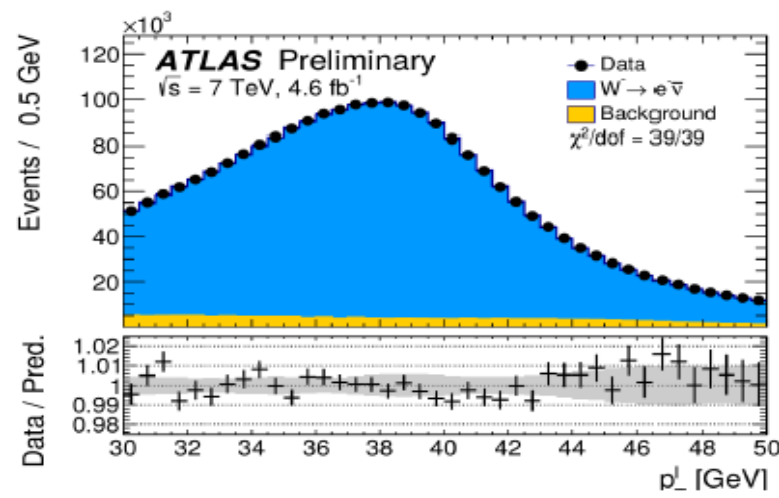
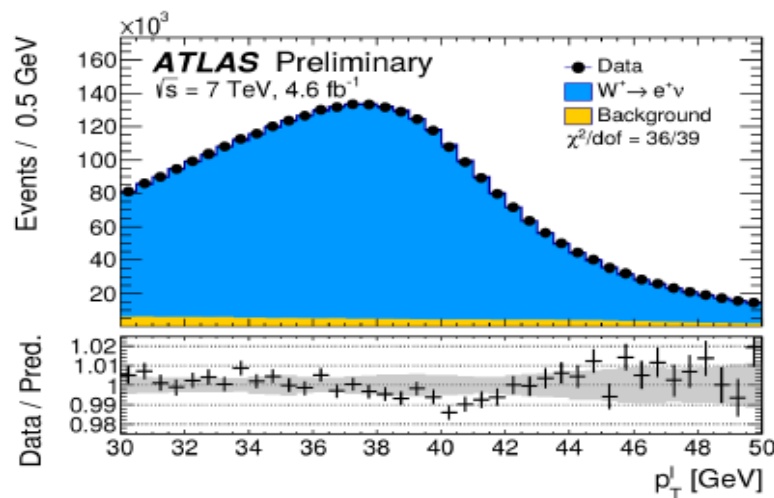


Results

Muons



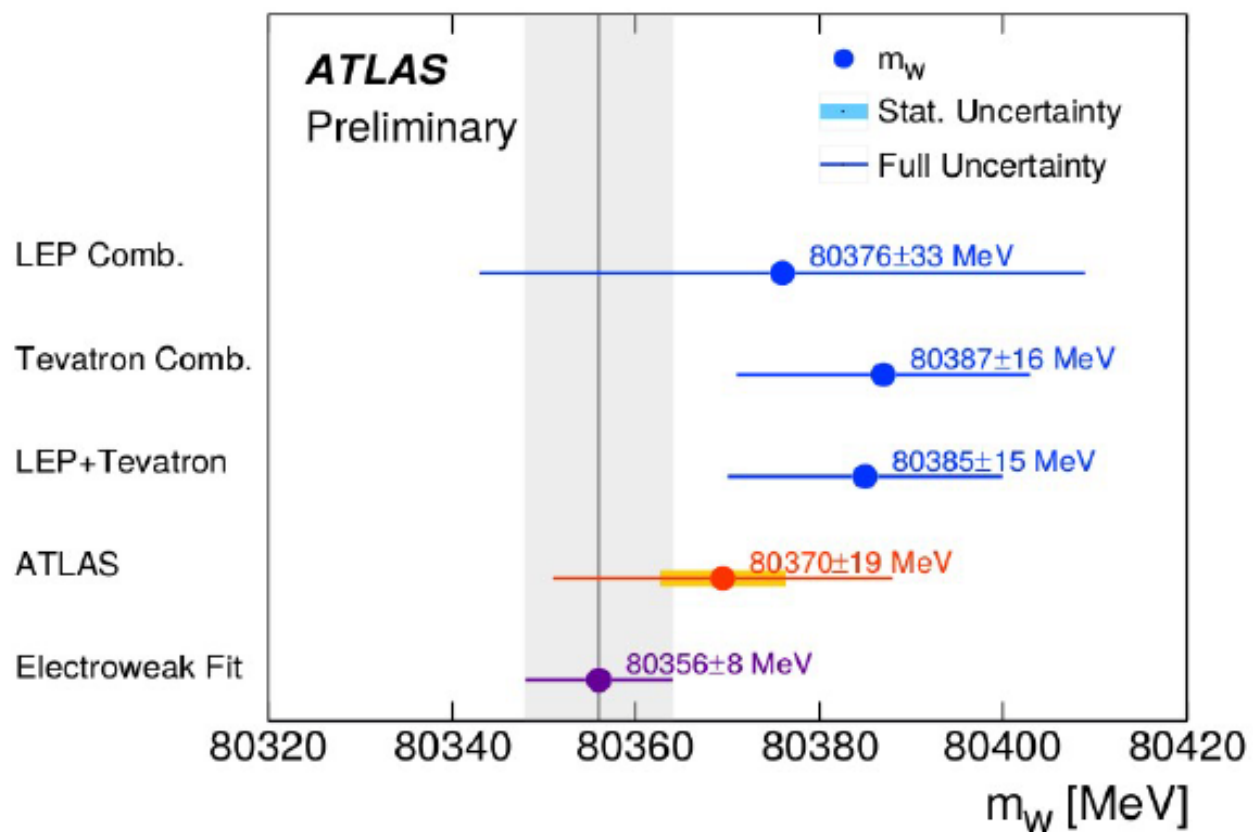
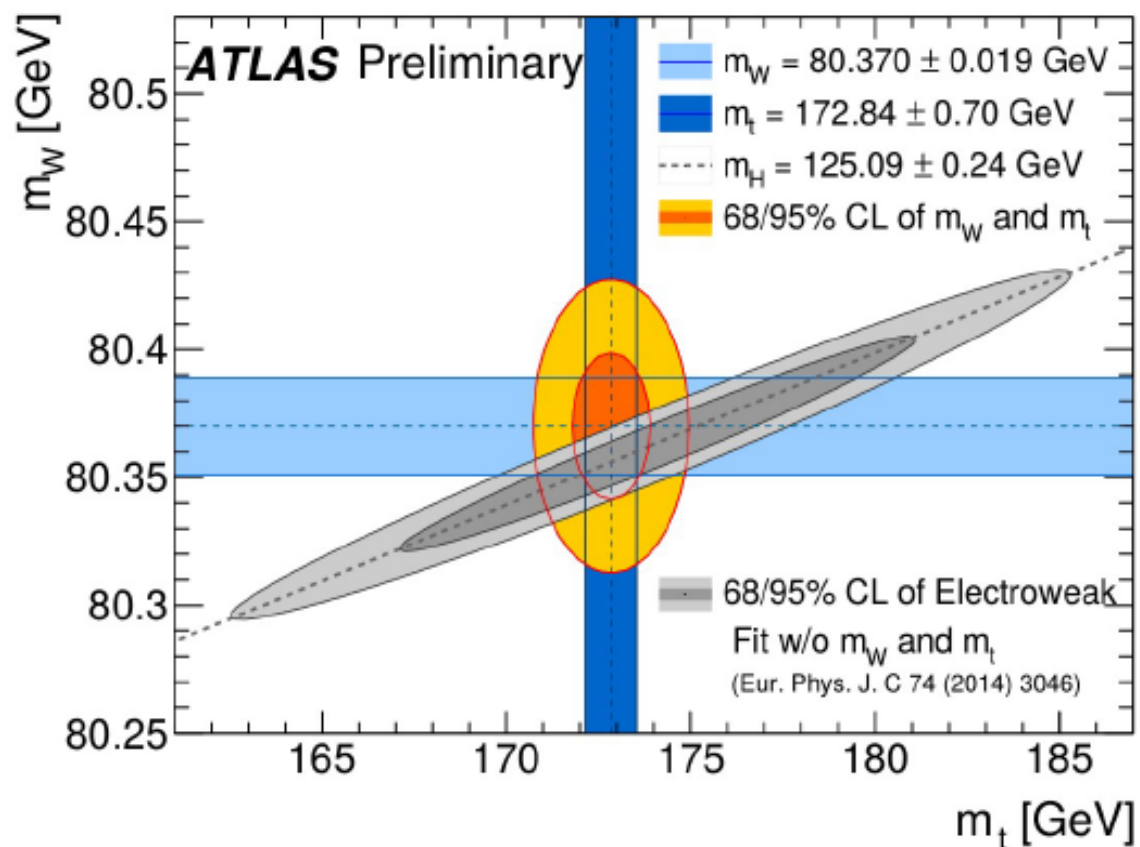
Electrons



(predictions set to the result of the combined m_W fit to all distributions)

Results

$$m_W = 80.370 \pm 0.007 \text{ (stat.)} \pm 0.011 \text{ (exp.syst.)} \pm 0.014 \text{ (mod.syst.) GeV}$$
$$= \underline{80.370 \pm 0.019 \text{ GeV}}$$

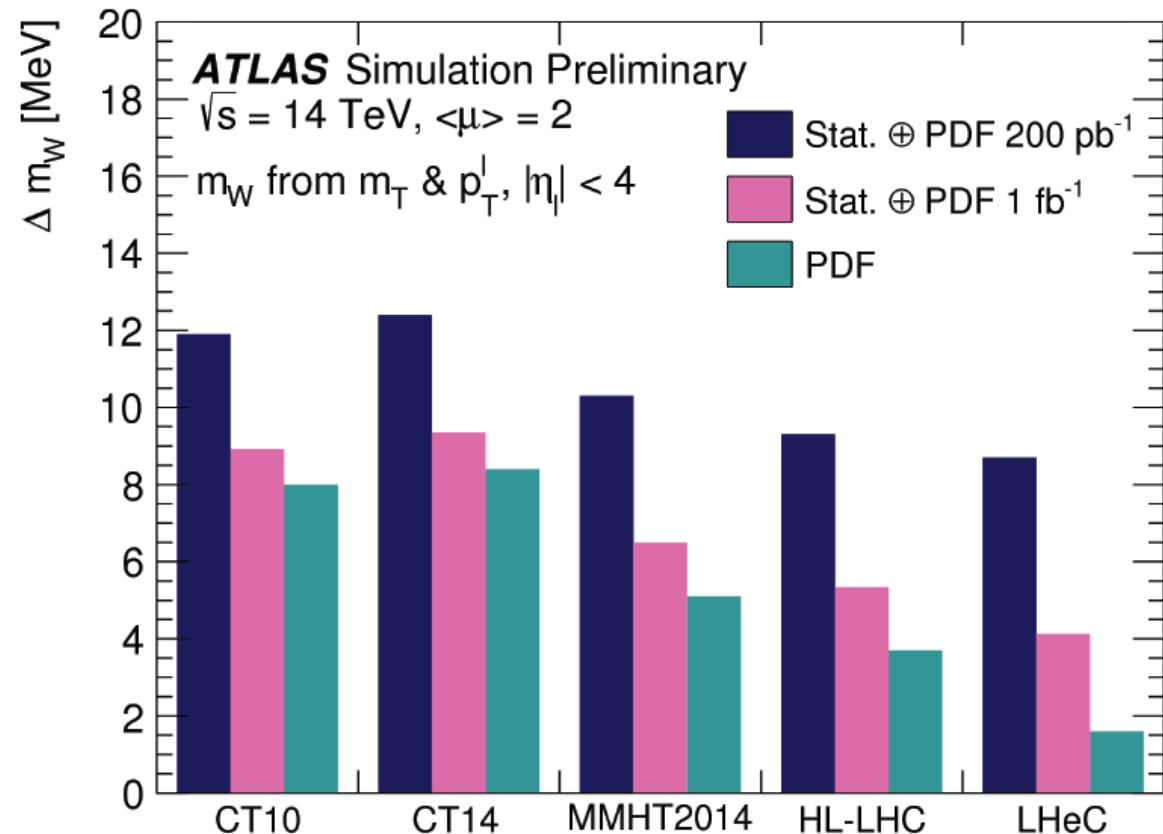


Prospects at the H-LHC

Potential low pile-up runs at HL-LHC (14 TeV) and HE-LHC (27 TeV): 200 pb⁻¹ per week, yielding ~1M candadite/week

Extended coverage with new tracking detector: $|\eta| < 4 \rightarrow$ 30% reduction of PDF uncertainties.

PDF uncertainties can be reduced to about 4 MeV using HL-LHC PDF sets, and to 2 MeV using inputs from a possible LHeC.

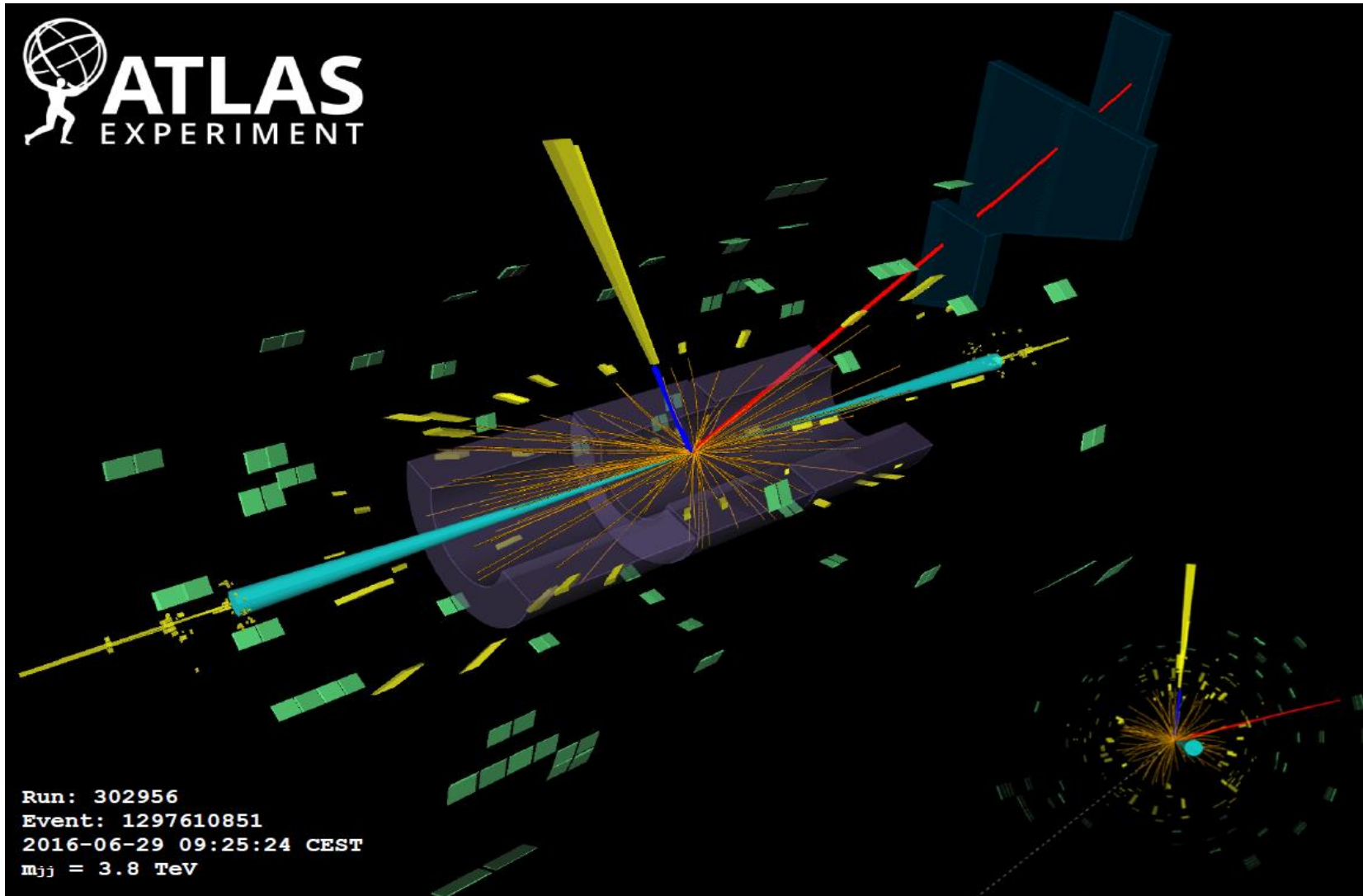


Weak boson interactions at high energy

$$pp \rightarrow \text{leptons/neutrinos} + jj + X$$

(following slides courtesy Philip Sommer)

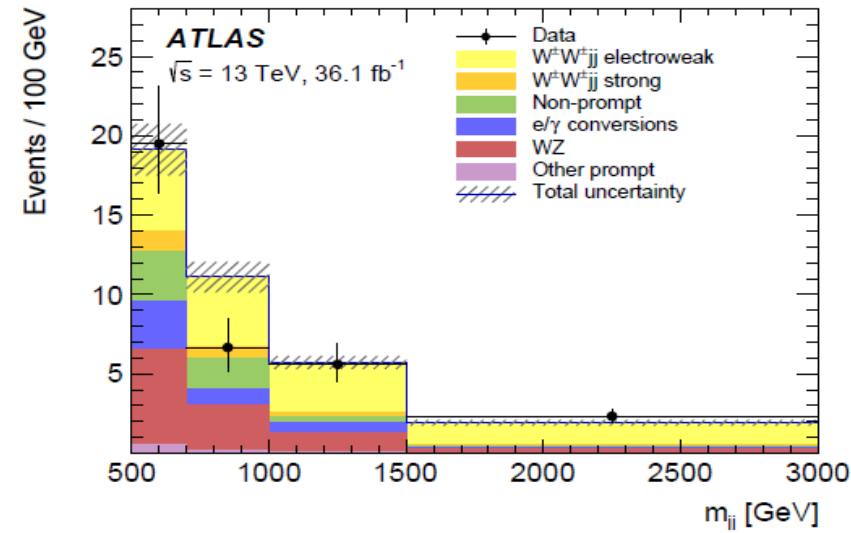
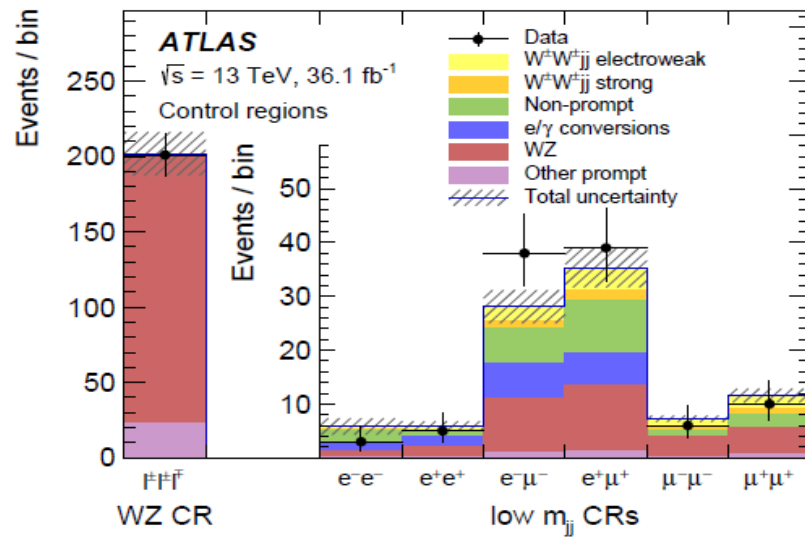
A spectacular signature :
2 or more leptons and two very forward, high- p_T jets



An electroweak $W^\pm W^\pm jj$ candidate event. The jets have $p_T=118 \text{ GeV}$ and $p_T=104 \text{ GeV}$, with $m_{jj}=3.8 \text{ TeV}$ and $\Delta y_{jj}=7.1$.

Observation of Electroweak $W^\pm W^\pm jj$ Production

arXiv:1906.03203



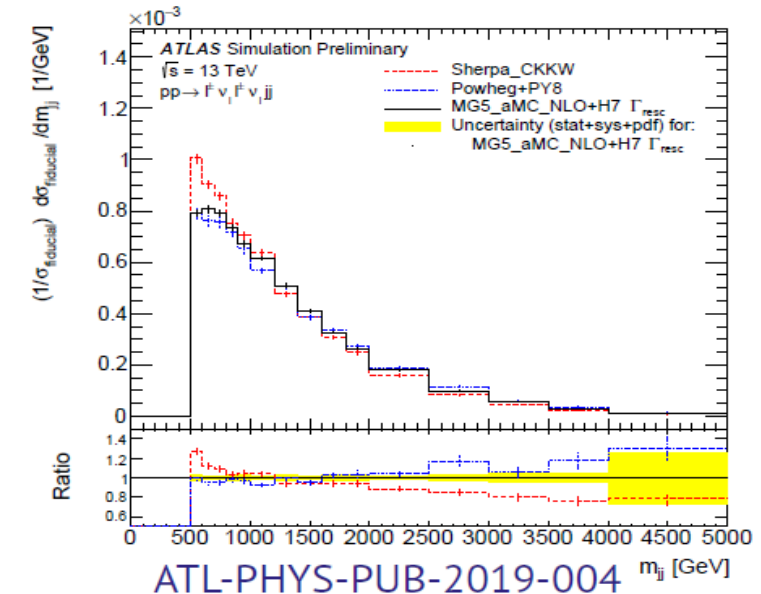
The analysis explores different background compositions in a likelihood fit to five bins in m_{jj} (by fitting e^+e^+ , e^-e^- , $e^+\mu^+$, $e^-\mu^-$, $\mu^+\mu^+$, $\mu^-\mu^-$ separately)

Separate bin to constrain $WZjj$ yield

$$0.86^{+0.07}_{-0.07} \text{ (stat.)}^{+0.18}_{-0.08} \text{ (exp. syst.)}^{+0.31}_{-0.23} \text{ (mod. syst.)}$$

Background-only hypothesis rejected with 6.5σ

(where 4.4σ and 6.5σ expected from Sherpa and PowhegBox+Pythia8, respectively)



ATL-PHYS-PUB-2019-004

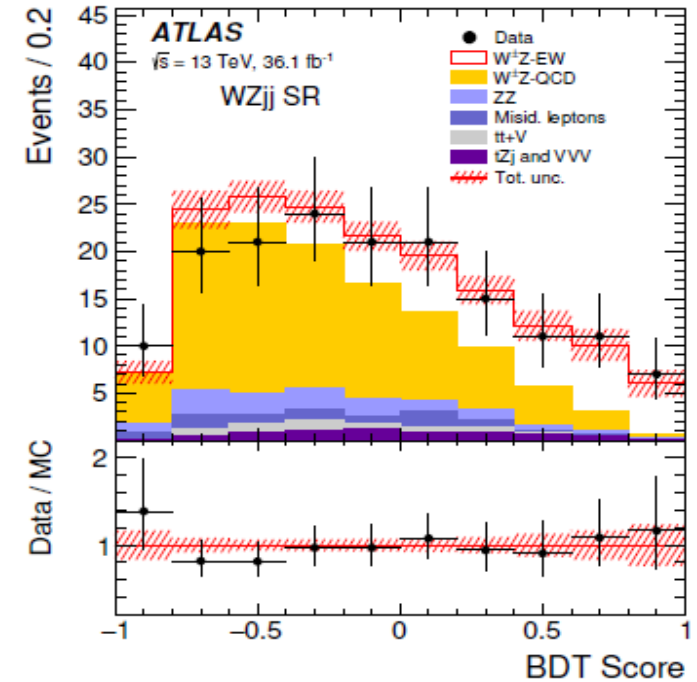
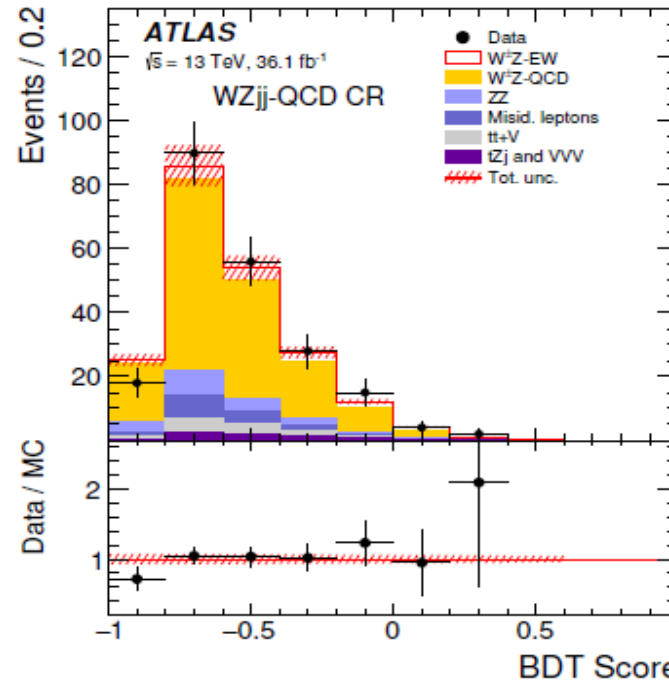
Observation of Electroweak $WZjj$ Production

Phys. Lett. B 793 (2019) 469

Signal extracted by fitting a BDT discriminant built from 15 variables

- ▶ jet kinematics
(m_{jj} , p_T^{j1} , p_T^{j2} , $\Delta\eta_{jj}$, $\Delta\phi_{jj}$, y^{j1} , n_{jets})
- ▶ diboson kinematics
(p_T^W , p_T^Z , η^W , $|y_Z - y_{e,W}|$, m_T^W)
- ▶ combined jet-diboson
($\Delta R(j_1, Z)$, $R_{p_T}^{\text{hard}}$, ζ_{lep})

Background constrained in three control regions



Overestimation of strong $WZjj$ production in Sherpa2.2.2, $\mu_{WZ-QCD} = 0.56 \pm 0.16$

Difference in electroweak $WZjj$ between Sherpa2.2.2 and MG5_aMC@NLO

Background only hypothesis rejected with 5.3σ (expected 3.2σ)

	SR	$WZjj$ -QCD CR	b -CR	ZZ -CR
Data	161	213	141	52
Total predicted	200 ± 41	290 ± 61	160 ± 14	45.2 ± 7.5
$WZjj$ -EW (signal)	24.9 ± 1.4	8.45 ± 0.37	1.36 ± 0.10	0.21 ± 0.12
$WZjj$ -QCD	144 ± 41	231 ± 60	24.4 ± 1.7	1.43 ± 0.22
Misid. leptons	9.8 ± 3.9	17.7 ± 7.1	30 ± 12	0.47 ± 0.21
$ZZjj$ -QCD	8.1 ± 2.2	15.0 ± 3.9	1.96 ± 0.49	35 ± 11
tZj	6.5 ± 1.2	6.6 ± 1.1	36.2 ± 5.7	0.18 ± 0.04
$t\bar{t} + V$	4.21 ± 0.76	9.11 ± 1.40	65.4 ± 10.3	2.8 ± 0.61
$ZZjj$ -EW	1.80 ± 0.45	0.53 ± 0.14	0.12 ± 0.09	4.1 ± 1.4
VVV	0.59 ± 0.15	0.93 ± 0.23	0.13 ± 0.03	1.05 ± 0.30

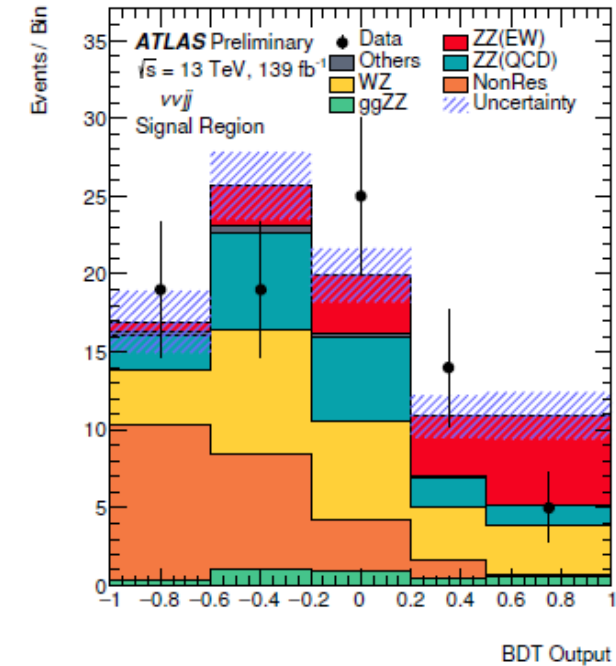
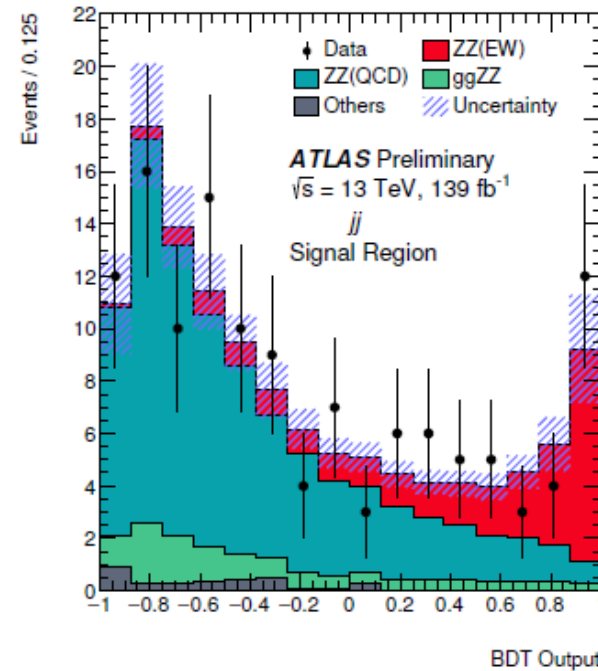
Event yields, pre-fit

Observation of $EW\ ZZjj$ Production

ATLAS-CONF-2019-033

The electroweak signal is extracted using a BDT with 12 (4ℓ) or 13 ($2\ell 2\nu$) variables

A fit of the BDT discriminant is performed simultaneously in $4\ell jj$ and $2\ell 2\nu jj$ (with a 4ℓ QCD CR defined by events failing Δy_{jj} or m_{jj})



Electroweak $ZZjj$ production is observed **for the first time** with the background-only hypothesis rejected with 5.5σ (expected 4.3σ from MG5_aMC@NLO)

The fiducial cross section is measured to be:

$$\sigma_{ZZjj-EW}^{\text{fid.}} = 0.82 \pm 0.21\text{ fb}$$

in agreement with the MG5_aMC@NLO prediction of $0.61 \pm 0.03\text{ fb}$

Summary

- After almost ten years of operation, the LHC is competing with the previous machines in electroweak precision.
- First measurements of m_W and $\sin^2\theta_{\text{eff}}^l$ match the earlier best individual measurements, and show the path for future iterations
- Vector boson interactions at high energy are probed for the first time, and will join the set of precision probes of EWSB in the mid term.